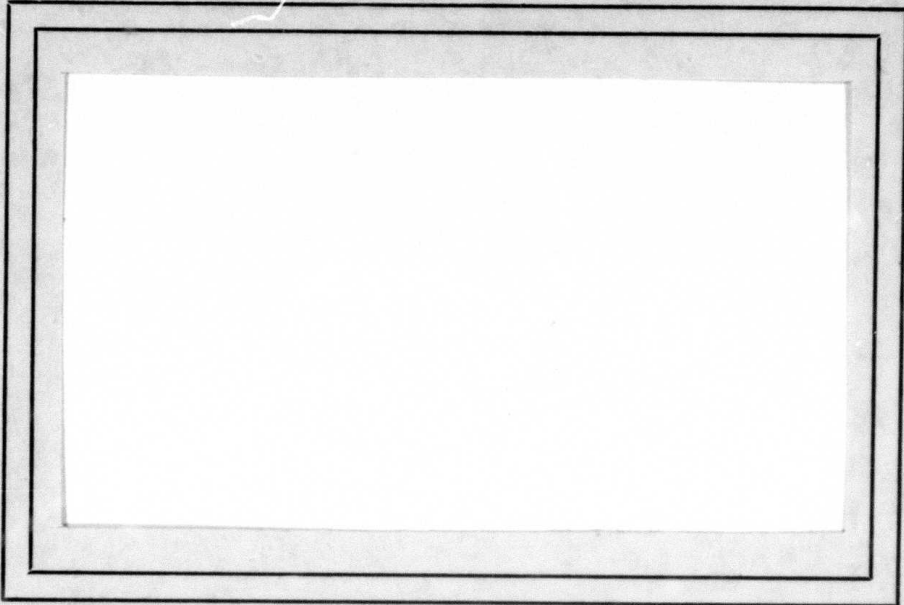


2

AD A 124809



DTIC
ELECTE
S FEB 24 1983 D
B

UNIVERSITY OF MARYLAND
COMPUTER SCIENCE CENTER

COLLEGE PARK, MARYLAND
20742

DISTRIBUTION STATEMENT A
Approved for public release;
Distribution Unlimited

DTIC FILE COPY

83 02 023 156

TR-1104
DAAG-53-76-C-0138/

September 1981

A COMPARATIVE STUDY OF
SEGMENTATION ALGORITHMS
FOR FLIR IMAGES

Ralph L. Hartley
Leslie J. Kitchen
Cheng-Ye Wang
Azriel Rosenfeld

Computer Vision Laboratory
Computer Science Center
University of Maryland
College Park, MD 20742

ABSTRACT

A comparative study of FLIR segmentation algorithms has been conducted in cooperation with Westinghouse Defense Systems Division. In the Maryland portion of the study, four techniques (two- and three-class relaxation, "pyramid linking", and "superspike") were tested on a Westinghouse-supplied database of 51 images obtained from NVL and other sources. (Two other techniques, "super-slice" and "pyramid spot detection", were rejected after preliminary studies.) The best technique, "superspike", extracted regions corresponding to over 88% of the targets, and had a false alarm rate of 1.6 false regions per true target.

The support of the Defense Advanced Research Projects Agency and the U.S. Army Night Vision Laboratory under Contract DAAG-53-76-C-0138 (DARPA Order 3206) is gratefully acknowledged, as is the help of Janet Salzman in preparing this paper.

DISTRIBUTION STATEMENT A

Approved for public release;
Distribution Unlimited

DTIC
ELECTE
FEB 24 1983
S D

B

1. Introduction

Under Contract DAAG-53-76-C-0138 (DARPA Order 3206) with the U.S. Army Night Vision and Electro-Optics Laboratory, the University of Maryland is conducting a study entitled "Understanding Features, Objects, and Backgrounds". The Westinghouse Defense Systems Division is participating as a subcontractor. The study is part of the DARPA Image Understanding Program, under the sponsorship of the DARPA Information Processing Technology Office (LTC Larry E. Druffel). Project monitor at USA NVEOL is Dr. George R. Jones. Principal investigator at Maryland is Prof. Azriel Rosenfeld, and at Westinghouse, Dr. Glenn E. Tisdale.

One phase of the research involves a comparative study of the effectiveness of segmentation algorithms in detecting tactical targets (tanks, trucks, etc.) in FLIR (Forward Looking InfraRed) imagery. This study has been conducted jointly by Maryland and Westinghouse. This report describes Maryland's part of the study; a report on Westinghouse's part is being issued concurrently.

Section 2 briefly describes the overall methodology of the study. Section 3 describes the techniques tested by Maryland. Section 4 presents the results of a pilot study using a few images, and Section 5 gives the results of the main study, using a database of 51 images supplied by Westinghouse. Section 6 discusses the results and outlines plans for future work.

2. Methodology

The overall approach used in the comparative study was as follows:

- 1) Each technique being tested (Section 3) was applied to the given set of images, yielding a classification of each image into subsets. Connected component labelling was performed on the resulting classified images, yielding a set of regions.
- 2) Regions that were too large, too small, or too elongated to be targets were eliminated. In our main study, the criteria for acceptability were

$$\left. \begin{array}{l} 4 \leq \text{height} \leq 41 \\ 3 \leq \text{width} \leq 50 \end{array} \right\} \text{ (pixels)}$$

$$0.4 \leq \text{aspect ratio} \leq 2.0$$

In addition, regions having the wrong polarity relative to the mean image gray level were eliminated.

- 3) For each surviving region, the coordinates of its centroid and the dimensions of its upright circumscribing rectangle were computed. The centroids and circumrectangles of the true targets were also known (from ground truth information and hand segmentation). A target was said to have been detected if the x and y displacements between a region centroid and a true target centroid were at most half the true target's rectangle dimensions. Region centroids not satisfying these conditions were considered

to be false alarms. The "segmentation accuracy" for each detected target was measured by the fraction of overlap between the circumrectangle of the detected region and that of the true target. Further details on this scoring process can be found in the companion Westinghouse report.



Accession For	
MMIS	<input checked="" type="checkbox"/>
MMIS	<input type="checkbox"/>
MMIS	<input type="checkbox"/>
By _____	
Distribution/	
Availability Codes	
Dist	Avail and/or Special
A	

3. Techniques

The following segmentation techniques were tested. The first two were rejected after a pilot study (Section 4); the remaining ones were used in the main study (Section 5). Brief descriptions of the techniques are given in the following paragraphs; for further details see the cited references.

3.1 Superslice [1]

This technique was developed during an earlier phase of the present project [2], and proved quite successful in FLIR object detection applications. A set of gray level thresholds is applied to the given image, and for each threshold, connected components of above-threshold points are extracted. The gray level gradient is also measured for the image, and points at which it is a local maximum are determined. A component is selected as a possible object if many gradient maxima coincide with its border and surround it.

3.2 Pyramid spot detection [2]

This technique was also developed earlier on this project; it extracts compact objects of arbitrary size from an image. We build an exponentially tapering "pyramid" of reduced-resolution versions of the image by successive block averaging, e.g., using nonoverlapping 2x2 blocks, or 4x4 blocks with 50% overlap in each direction, so that each image is half the size ($\frac{1}{4}$ the area) of the preceding. At each level of the pyramid,

we apply a standard spot-detection operator - e.g., we compare each pixel to its eight neighbors, and judge a spot to be present if they differ sufficiently. A spot that is detected in this way should correspond to a compact object on a contrasting background in the original image. For each such spot, we consider the portion of the original image corresponding to the pixel and its neighbors, and apply a threshold to this portion, chosen midway between the gray level of the pixel (an average of a block of gray levels in the original image) and the average gray level of its neighbors (an average of block averages). This thresholding generally extracts the object that gave rise to the spot detection.

3.3 Relaxation [4,5]

"Relaxation" methods of object extraction were also extensively studied earlier on this project. The basic approach is to initially assign "object" and "background" probabilities to each pixel, based on their gray levels. The probabilities are then iteratively adjusted based on the probabilities of the neighboring pixels, with like reinforcing like. When this is done, the probabilities tend to converge to relative certainty ((0,1) or (1,0)), and yield a good segmentation of the image into objects and background. A refinement, studied by Westinghouse, makes use of three rather than two classes - "object", "background", and "clutter".

3.4 Pyramid linking [6]

A method of segmenting an image based on creating links between pixels at successive levels of a "pyramid" has been under study at our laboratory for the past year. We build the pyramid using overlapping 4×4 blocks; thus each pixel has 16 "sons" (on the level below) that contribute to its average, and four "fathers" (on the level above) to whose average it contributes. We now link each pixel to the father whose value (=average) is closest to its own. We then recompute the averages, allowing only those sons that are linked to a pixel to contribute to its average. We now change the links based on these new averages, then recompute the averages again, and so on. This process stabilizes after a few iterations; at this stage the links define subtrees of the pyramid, rooted at the top level, which we take to be 2×2 , so that there are (at most) four trees. The sets of leaves of these trees (pixels in the original image) thus define a segmentation of the original image into at most four subsets.

3.5 "Superspike" [7]

A powerful method of image smoothing based on iterated selective local averaging was recently developed at our laboratory. Each pixel is averaged with those of its neighbors that satisfy the following criteria, based on the image's histogram:

- a) The neighbor is more probable than the pixel, i.e., its gray level has a higher value in the histogram.

b) The histogram has no concavity between the gray levels of the pixel and the neighbor (as would be the case if they belonged to two different peaks, or to a peak and a shoulder).

When this process is iterated a few times, the histogram generally turns into a small set of spikes. The image can then be segmented by mapping each pixel into the nearest spike. In our experiments we eliminated small spikes, mapping them into nearby taller ones, until only five spikes remained, thus segmenting the image into five subsets.

4. Pilot study

In a pilot study, all six techniques (including both two-class and three-class relaxation) were applied to three image samples (see Figure 1) chosen from the NVL Fort Polk I data base. Figure 1 also shows the resulting segmented images. We see that the pyramid spot technique did not perform very well. This is not too surprising, since this technique was designed for the extraction of isolated objects on a contrasting background [3]. Results with the relaxation, pyramid linking, and superspike techniques looked more promising, and it was therefore decided to use all of them in the main study. The superslice technique was not used in the main study because of its comparatively high computational cost.

5. Main study

The main study used a data base of 51 FLIR images supplied by Westinghouse. These images were from four sources:

<u>Image Nos.</u>	<u>Source</u>
2-10	Navy (China Lake)
11-30	NVL data
31-36	Air Force, TASVAL
55-70	NVL flight test

All images are 128×128; nos. 21-30 were obtained from 64×64 images by horizontal and vertical reflection, in order to present the targets in four orientations. For a more detailed description of the data base, see the companion Westinghouse report. The images are shown in Figure 2.

The four selected techniques (two- and three-class relaxation, pyramid linking, and superspike) were applied to these images. [In the case of images 21-30, they were applied to only one quadrant, since the methods are essentially orientation-invariant; the scores (detections and false alarms) obtained in this way were multiplied by 4.] The pyramid linking algorithm was designed for 64×64 images; in order to apply it to images 2-10, 31-36, and 55-70, they were resampled down to that size, and the outputs (centroids and rectangles) were scaled up in order to compare them with the ground truth.

Figure 3 shows the segmentation results using the four methods for each of the 51 images. Table 1 lists the parameters (centroid coordinates C_i, C_j and rectangle dimensions R_i, R_j) for the 126 targets actually present in the images, and Tables 2-5 list these parameters for the targets (and false alarms) detected by each of the methods. Tables 6-9 show, for each method and each image, the number of targets correctly detected, the number of extra detections (centroid of more than one detected object lies in the inner half of a true target's rectangle), the number of false alarms, and the segmentation accuracy. Those results are summarized in Table 10 for all four methods and for the four classes of images.

We see from these results that segmentation accuracy does not vary greatly among the methods; it ranges between about .5 and .8 in all cases. Extra detections are also not a significant factor, except perhaps for the pyramid linking and superspike methods as applied to the NVL data (images 11-30). As regards correct detections and false alarms, 3-class relaxation and superspike were the best methods (though no method was very good) for the Navy images; pyramid linking and superspike had good detection rates for the NVL data, but the former had a much higher false alarm rate; and superspike was by far the best method for the Air Force and NVL flight test images, making it the best method overall. It detected 111 of the 126 targets (over 88%) with only 26 extra detections and 202 false alarms

(about 1.6 per true target), and its segmentation accuracy was a reasonable 0.66. The next best method, pyramid linking (which, it should be recalled, was applied to half-resolution versions of images nos. 2-10, 31-36, and 55-70), detected only 63% of the targets and had many more false alarms (over 5 per target).

6. Concluding remarks

The results of the main study show that one method, "superspike", performed substantially better on the Westinghouse data base than the other methods tested. It detected nearly 90% of the true targets and gave only 1.6 false alarms per target. On the NVL imagery alone its performance was even better. Note that these results were obtained using segmentation alone, in conjunction with very crude size and aspect criteria. If the segmentation step were followed by a classification algorithm, much better performance could be expected.

Some further improvement in performance can undoubtedly be obtained by further refining the segmentation process. However, there are limits to what can be achieved in this way by algorithms that incorporate so little knowledge about the nature of the targets. In order to attain a significantly higher level of performance, it will probably be necessary to develop a knowledge-driven system capable of some degree of reasoning about the regions extracted by the initial segmentation. An approach to such a system is currently under investigation and will be described in a future report.

References

1. D. L. Milgram, Region extraction using convergent evidence, Computer Graphics Image Processing 11, 1979, 1-12.
2. D. L. Milgram and A. Rosenfeld, Algorithms and Hardware Technology for Image Recognition, Final Report, Computer Vision Laboratory, Computer Science Center, University of Maryland, College Park, MD, March 31, 1978.
3. M. Shneier, Using pyramids to define local thresholds for blob detection, TR-808, Computer Vision Laboratory, Computer Science Center, University of Maryland, College Park, MD, September 1979.
4. R. C. Smith, A general-purpose software package for array relaxation, TR-839, Computer Vision Laboratory, Computer Science Center, University of Maryland, College Park, MD, December 1979.
5. R. C. Smith and A. Rosenfeld, Thresholding using relaxation, IEEE Trans. Pattern Analysis Machine Intelligence 3, 1981, 598-606.
6. P. Burt, T. H. Hong, and A. Rosenfeld, Segmentation and estimation of image region properties through cooperative hierarchical computation, TR-927, Computer Vision Laboratory, Computer Science Center, University of Maryland, College Park, MD, August 1980; to appear in IEEE Trans. Systems, Man, Cybernetics.
7. K. A. Narayanan and A. Rosenfeld, Image smoothing by local use of global information, TR-1006, Computer Vision Laboratory, Computer Science Center, University of Maryland, College Park, MD, February 1981.

<u>Image No.</u>	<u>True Target (s)</u>			
	<u>Ci</u>	<u>Cj</u>	<u>Ri</u>	<u>Rj</u>
2	19.5	92.5	9.0	5.0
	51.5	91.5	5.0	4.0
	95.5	89.0	7.0	3.5
3	58.0	67.5	3.0	2.0
	74.5	102.0	2.0	1.5
4	-	-	-	-
5	-	-	-	-
6	-	-	-	-
7	-	-	-	-
8	57.5	86.5	2.0	4.0
	74.5	74.0	3.0	2.5
9	41.5	92.5	4.0	4.0
10	-	-	-	-
11	57.5	19.0	3.0	6.5
12	36.5	35.5	5.0	12.0
13	40.5	37.0	6.0	12.5
14	31.0	36.0	14.5	18.5
15	28.5	40.0	14.0	20.5
16	28.5	42.0	6.0	10.5
17	36.0	31.5	11.5	17.0
18	42.0	36.0	13.5	17.5
19	37.0	35.0	18.5	18.5
20	33.0	48.0	17.5	14.5
21	32.5	39.5	17.0	18.0
22	45.5	31.5	17.0	17.0

Table 1. True targets in each image

<u>Image No.</u>	<u>True Target (s)</u>			
	<u>Ci</u>	<u>Cj</u>	<u>Ri</u>	<u>Rj</u>
23	38.5	34.5	13.0	23.0
24	37.0	37.0	13.5	22.5
25	41.0	46.0	10.5	13.5
26	27.0	35.5	9.5	14.0
27	31.0	25.5	17.0	14.0
28	29.5	27.5	14.0	14.0
29	27.5	42.0	14.0	11.5
30	43.0	42.0	9.5	9.5
31	60.5	75.0	7.0	12.0
32	62.0	71.5	7.5	14.0
33	71.0	59.5	12.5	17.0
34	64.5	75.0	11.0	22.5
35	56.0	63.5	13.5	19.0
36	67.5	70.0	14.0	15.5
55	83.5	81.5	3.5	7.0
	85.5	105.5	3.0	6.0
56	84.0	78.0	3.5	7.5
	85.0	106.5	2.5	5.0
57	91.0	74.5	3.5	8.0
	93.5	106.5	3.0	5.0
58	102.0	72.5	4.5	9.0
	103.5	108.0	3.0	5.5
59	96.0	68.5	4.5	11.0
	98.5	110.0	4.0	7.5
60	86.0	52.5	5.5	13.0
	88.5	103.0	5.0	8.5

Table 1, cont'd.

<u>Image No.</u>	<u>True Target (s)</u>			
	<u>Ci</u>	<u>Cj</u>	<u>Ri</u>	<u>Rj</u>
61	76.5	14.5	7.0	14.5
	78.0	76.0	6.5	11.5
62	90.0	18.5	11.5	18.5
	94.0	98.5	8.5	15.0
63	84.5	4.0	2.0	4.0
	84.0	19.5	2.5	4.0
64	85.0	5.0	2.5	5.0
	84.5	25.5	3.0	4.0
65	93.5	9.5	3.5	7.0
	95.5	31.5	2.0	4.0
66	102.5	14.5	4.0	8.0
	103.0	40.0	2.5	4.5
67	100.0	24.0	4.5	10.5
	102.0	53.0	3.5	5.5
68	90.0	24.0	5.5	11.5
	91.5	61.0	3.0	6.5
69	78.5	12.0	7.0	12.0
	79.5	56.5	4.0	8.0
70	96.5	54.5	9.5	19.0
	97.5	118.0	4.0	10.5

Table 1, cont'd.

<u>Image No.</u>	<u>Target(s) detected by 2-class relaxation</u>			
	<u>C_i</u>	<u>C_j</u>	<u>R_i</u>	<u>R_j</u>
2	12.5	121.0	6.0	7.5
	15.5	6.5	9.0	6.0
	53.0	72.0	8.5	9.5
3	14.5	83.0	14.0	23.5
4	16.0	57.5	15.5	13.0
	28.0	10.5	15.5	9.0
	29.0	25.5	2.5	2.0
	39.5	56.0	4.0	3.5
5	25.5	66.0	6.0	9.5
	87.5	40.0	3.0	3.5
	90.0	60.5	8.5	8.0
	103.5	110.5	10.0	11.0
	103.5	22.5	16.0	22.0
	121.0	88.0	7.5	11.5
6	-	-	-	-
7	5.0	44.5	4.5	11.0
	33.5	11.5	10.0	11.0
	32.0	126.0	4.5	2.5
	62.5	37.5	5.0	4.0
	79.0	10.5	19.5	10.0
	118.5	48.0	10.0	21.5
8	3.0	11.0	2.5	5.5
9	8.0	17.0	7.5	5.5
	5.0	40.0	3.5	3.5
	17.5	71.5	2.0	2.0
	20.0	64.0	5.5	4.5
	25.0	81.5	2.5	2.0
	37.5	75.0	7.0	11.5
	33.0	94.0	12.5	7.5
	40.5	34.0	3.0	3.5
	53.0	123.5	2.5	4.0
	57.0	3.0	4.5	2.5
	72.5	94.5	2.0	2.0
	77.5	7.5	2.0	2.0
	70.5	116.0	11.0	12.5
79.0	95.0	2.5	5.5	
91.0	66.5	3.5	4.0	

Table 2. Targets detected by 2-class relaxation in each image

Image No. Target(s) detected by 2-class relaxation

	<u>Ci</u>	<u>Cj</u>	<u>Rj</u>	<u>Ri</u>
10	6.5	14.5	2.0	3.0
	13.0	110.0	12.5	18.5
	34.5	71.0	14.0	14.5
	59.0	4.5	3.5	4.0
	51.5	39.0	10.0	9.5
	101.5	25.0	8.0	5.5
	100.5	6.5	2.0	2.0
11	34.5	45.0	3.0	4.5
	39.5	33.0	3.0	2.5
12	26.0	4.0	3.5	3.5
13	16.5	57.0	3.0	6.5
	39.0	8.5	6.5	8.0
14	27.0	35.5	20.5	20.0
15	27.5	39.5	17.0	25.0
16	15.0	29.5	2.5	2.0
	15.5	37.0	2.0	2.5
	16.5	7.0	2.0	2.5
	28.5	42.5	7.0	11.0
	32.5	12.0	4.0	7.5
17	-	-	-	-
18	3.0	36.5	2.5	2.0
	7.0	52.5	6.5	12.0
19	-	-	-	-
20	-	-	-	-
21	33.0	39.5	17.5	19.0
22	45.5	31.5	19.0	18.0
23	61.5	6.0	3.0	5.5
24	37.5	39.5	16.0	25.0
25	-	-	-	-

Table 2, cont'd.

Image No. Target(s) detected by 2-class relaxation

	<u>Ci</u>	<u>Cj</u>	<u>Ri</u>	<u>Rj</u>
26	2.5	24.0	2.0	2.5
	26.5	35.5	11.0	15.0
27	32.0	26.0	18.5	15.5
	49.5	4.0	2.0	3.5
28	3.0	41.0	2.5	5.5
	4.5	22.5	2.0	4.0
	6.5	9.5	3.0	6.0
	33.0	23.0	19.5	22.5
	49.5	5.5	3.0	2.0
	49.0	12.5	3.5	3.0
29	31.5	42.0	19.0	15.5
	47.5	21.0	4.0	3.5
	59.0	10.0	5.5	3.5
30	38.0	61.0	4.5	3.5
	60.5	28.5	4.0	2.0
31	6.5	11.5	5.0	11.0
	60.5	75.0	9.0	13.5
	103.0	49.0	4.5	8.5
32	52.5	43.5	3.0	3.0
	74.0	123.0	10.5	5.5
	123.5	17.0	4.0	7.5
33	71.0	60.5	13.5	20.0
34	14.5	84.0	3.0	4.5
35	51.5	108.5	19.0	20.0
	62.5	23.0	2.0	2.5
	76.5	81.5	2.0	3.0
36	-	-	-	-
55	-	-	-	-
56	-	-	-	-
57	-	-	-	-
58	-	-	-	-

Table 2, cont'd.

<u>Image No.</u>	<u>Target(s) detected by 2-class relaxation</u>			
	<u>Ci</u>	<u>Cj</u>	<u>Ri</u>	<u>Rj</u>
59	-	-	-	-
60	20.0	120.5	3.5	8.0
61	60.5	122.0	7.0	6.5
	81.0	75.5	10.5	12.0
	110.5	114.5	7.0	9.0
62	93.5	99.0	11.0	15.5
	112.0	85.5	3.5	8.0
63	-	-	-	-
64	-	-	-	-
65	-	-	-	-
66	100.5	84.5	2.0	4.0
67	-	-	-	-
68	-	-	-	-
69	-	-	-	-
70	82.5	2.5	3.0	2.0

Table 2, cont'd.

<u>Image No.</u>	<u>Target(s) detected by 3-class relaxation</u>			
	<u>Ci</u>	<u>Cj</u>	<u>Ri</u>	<u>Rj</u>
2	17.5	92.5	11.0	6.0
	16.5	6.0	8.0	5.5
	41.0	22.5	2.5	2.0
	51.5	96.0	7.0	9.5
	52.5	122.0	12.0	6.5
	51.5	74.5	5.0	5.0
	98.5	71.5	6.0	5.0
	97.0	16.0	7.5	8.5
	106.0	67.5	2.5	3.0
3	4.5	67.0	3.0	3.5
	40.5	114.5	3.0	2.0
	64.5	44.5	5.0	5.0
	72.5	124.5	5.0	3.0
	76.5	12.5	11.0	11.0
	79.5	66.0	12.0	10.5
	80.5	84.0	5.0	7.5
	103.5	105.5	8.0	7.0
	4	6.0	58.0	4.5
14.5		108.0	13.0	19.5
25.5		10.5	12.0	8.0
29.0		25.5	5.5	5.0
31.5		2.5	4.0	2.0
35.5		10.5	10.0	6.0
54.5		72.5	3.0	2.0
72.5		84.5	4.0	3.0
5		86.5	40.0	2.0
	90.0	61.5	8.5	10.0
	103.5	110.5	10.0	11.0
	103.5	22.5	16.0	22.0
	121.0	87.5	7.5	11.0
6	64.5	36.0	2.0	3.5
7	34.5	12.5	11.0	12.0
	63.0	38.0	5.5	5.5
	71.5	74.0	4.0	4.5
	95.5	26.5	2.0	2.0
	95.5	119.0	12.0	8.5
	111.0	121.5	2.5	6.0
	119.5	38.0	2.0	4.5
	121.5	117.5	2.0	3.0
	113.5	100.0	12.0	19.5
118.0	47.0	10.5	22.5	

Table 3. Targets detected by 3-class relaxation in each image.

Image No. Target(s) detected by 3-class relaxation

8	30.5	8.0	7.0	6.5
	44.5	23.5	3.0	5.0
	65.5	78.0	2.0	4.5
	72.5	49.0	9.0	21.5
	80.5	80.0	3.0	5.5
	83.5	114.5	8.0	13.0
	99.5	20.5	2.0	2.0
	117.5	4.5	4.0	4.0
	124.0	4.0	4.5	3.5
	124.5	112.0	3.0	4.5
	9	5.5	16.5	4.0
13.5		19.5	2.0	2.0
13.0		85.5	2.5	3.0
21.0		114.5	19.5	14.0
36.5		67.5	3.0	3.0
40.5		92.0	5.0	4.5
37.0		79.0	4.5	4.5
89.5		16.5	10.0	9.0
87.5		33.5	6.0	7.0
91.5		100.0	2.0	3.5
10		16.0	111.0	8.5
	35.0	71.0	13.5	13.5
	50.5	40.0	5.0	7.5
	56.0	117.0	2.5	3.5
	60.0	4.0	2.5	2.5
	58.5	35.0	2.0	2.5
	80.0	24.0	2.5	2.5
	117.5	37.0	2.0	2.5
11	19.5	59.0	2.0	2.5
	56.5	13.0	7.0	12.5
	53.5	47.5	9.0	15.0
12	36.5	40.5	3.0	4.0
	54.5	61.5	3.0	2.0
13	13.0	56.0	9.5	7.5
	25.5	56.5	2.0	2.0

Table 3, cont'd.

<u>Image No.</u>	<u>Target(s) detected by 3-class relaxation</u>			
	<u>Ci</u>	<u>Cj</u>	<u>Ri</u>	<u>Rj</u>
14	25.5	40.5	2.0	2.0
	29.5	39.0	5.0	7.5
	36.5	43.5	4.0	6.0
15	-	-	-	-
16	7.0	50.5	2.5	3.0
	15.5	32.0	4.0	9.5
	16.5	18.5	3.0	3.0
	15.5	7.0	4.0	6.5
	22.5	46.5	13.0	17.0
	34.0	12.0	12.5	9.5
17	-	-	-	-
18	3.0	37.0	2.5	3.5
	7.5	52.5	7.0	11.0
	26.0	57.5	2.5	2.0
19	-	-	-	-
20	-	-	-	-
21	33.5	40.0	20.0	23.5
22	2.5	18.5	2.0	4.0
	13.5	19.5	2.0	3.0
	15.0	11.0	14.5	10.5
	32.5	2.5	3.0	2.0
23	4.0	10.0	3.5	2.5
	11.0	3.5	5.5	3.0
24	-	-	-	-
25	-	-	-	-
26	4.5	6.0	2.0	2.5
27	29.0	24.5	13.5	12.0
28	30.0	26.5	14.5	16.0
29	-	-	-	-
30	9.5	55.0	2.0	2.5

Table 3, cont'd.

Image No. Target(s) detected by 3-class relaxation

	<u>Ci</u>	<u>Cj</u>	<u>Ri</u>	<u>Rj</u>
31	6.5	11.0	4.0	9.5
	7.0	12.0	5.5	11.5
	37.5	65.5	2.0	2.0
	60.5	74.5	7.0	11.0
	66.0	126.0	3.5	2.5
	113.5	38.0	2.0	3.5
	116.5	6.0	3.0	4.5
	123.5	125.5	2.0	3.0
32	50.0	40.0	6.5	8.5
	56.0	25.5	2.5	3.0
	59.5	71.0	9.0	12.5
	74.0	121.5	11.5	7.0
	72.5	125.0	5.0	2.5
	122.5	15.0	6.0	11.5
33	39.0	97.0	6.5	5.5
	40.0	84.5	7.5	9.0
	64.5	35.5	3.0	5.0
	66.5	55.0	9.0	14.5
	68.5	59.5	8.0	17.0
	95.5	110.5	13.0	17.0
	113.0	110.5	3.5	4.0
	115.5	96.0	3.0	3.5
	119.5	102.0	2.0	3.5
	123.0	89.5	4.5	5.0
	123.5	114.0	2.0	4.5
	125.0	99.0	2.5	3.5
34	14.5	84.0	3.0	4.5
35	51.5	108.5	19.0	20.0
	62.5	23.0	2.0	2.5
	76.5	81.5	2.0	3.0
36	73.5	54.5	3.0	3.0
55	-	-	-	-
56	73.5	54.5	3.0	3.0
57	91.5	75.0	3.0	6.5
	93.5	109.0	2.0	2.5

Table 3, cont'd.

Image No. Target(s) detected by 3-class relaxation

	<u>Ci</u>	<u>Cj</u>	<u>Rj</u>	<u>Ri</u>
58	101.5	72.0	4.0	8.5
	103.0	110.5	2.5	3.0
	117.5	125.5	3.0	3.0
59	96.0	68.5	4.5	10.0
	99.5	112.0	3.0	5.5
	104.5	126.0	2.0	2.5
60	86.5	52.5	6.0	12.0
	89.5	104.0	4.0	7.5
	116.0	125.5	4.5	3.0
61	77.0	15.0	7.5	13.5
	79.0	76.0	4.5	9.5
62	63.5	105.0	2.0	2.5
	70.0	123.0	3.5	5.5
	91.0	17.5	10.5	16.0
	96.0	98.5	6.5	14.0
	93.5	99.0	12.0	16.5
63	22.5	107.0	7.0	16.5
	27.5	105.5	3.0	5.0
	26.5	126.5	2.0	2.0
	37.5	26.0	2.0	4.5
64	-	-	-	-
65	-	-	-	-
66	90.5	126.0	3.0	2.5
	93.0	116.5	2.5	4.0
67	100.5	29.5	2.0	2.0
68	90.0	32.0	2.5	2.5
69	17.5	121.0	5.0	7.5
	47.5	35.0	2.0	3.5
	78.0	20.0	3.5	3.5
70	82.5	2.5	3.0	2.0
	95.5	68.5	5.0	5.0
	96.5	43.5	2.0	2.0

Table 3, cont'd.

Image No. Target(s) detected by pyramid linking

	<u>Ci</u>	<u>Cj</u>	<u>Ri</u>	<u>Rj</u>
2	6.5	5.5	6.0	5.0
	17.5	5.5	7.0	5.0
	10.5	118.5	10.0	10.0
	16.5	108.5	2.0	2.0
	35.5	106.5	3.0	4.0
	40.5	22.5	4.0	2.0
	43.5	71.5	11.0	11.0
	52.5	97.5	10.0	11.0
	52.5	74.5	6.0	6.0
	62.5	60.5	4.0	4.0
	87.5	26.5	3.0	2.0
	84.5	101.5	4.0	3.0
	90.5	18.5	4.0	4.0
	98.5	8.5	8.0	6.0
	97.5	15.5	7.0	7.0
	108.5	121.5	6.0	7.0
	107.5	97.5	7.0	5.0
	116.5	107.5	2.0	3.0
	123.5	2.5	3.0	2.0
	115.5	15.5	13.0	15.0
3	2.5	43.5	2.0	3.0
	14.5	77.5	14.0	17.0
	8.5	39.5	4.0	3.0
	10.5	108.5	6.0	4.0
	14.5	34.5	2.0	4.0
	17.5	21.5	5.0	7.0
	62.5	43.5	8.0	5.0
	68.5	121.5	8.0	7.0
	74.5	12.5	12.0	12.0
	78.5	17.5	4.0	5.0
	85.5	8.5	7.0	4.0
	80.5	73.5	14.0	19.0
	105.5	108.5	9.0	12.0
	105.5	44.5	3.0	6.0
	103.5	30.5	5.0	4.0
4	11.5	103.5	11.0	7.0
	27.5	10.5	11.0	6.0
	18.5	118.5	2.0	2.0
	20.5	112.5	2.0	2.0
	39.5	82.5	7.0	4.0
	54.5	73.5	8.0	5.0
	74.5	98.5	6.0	4.0
	106.5	41.5	4.0	3.0
	117.5	38.5	11.0	8.0

Table 4. Targets detected by pyramid linking in each image.

Image No. Target(s) detected by pyramid linking

	<u>Ci</u>	<u>Cj</u>	<u>Ri</u>	<u>Rj</u>
5	4.5	79.5	4.0	7.0
	8.5	120.5	8.0	8.0
	11.5	21.5	9.0	21.0
	19.5	61.5	3.0	5.0
	19.5	80.5	3.0	4.0
	64.5	7.5	8.0	7.0
	78.5	19.5	16.0	19.0
	74.5	115.5	8.0	13.0
	79.5	44.5	5.0	4.0
	89.5	46.5	3.0	4.0
	110.5	4.5	6.0	4.0
	116.5	19.5	10	9.0
	118.5	97.5	2.	3.0
	123.5	103.5	5.0	9.0
	125.5	113.5	3.0	7.0
6	10.5	62.5	2.0	4.0
	11.5	70.5	3.0	4.0
	30.5	88.5	2.0	2.0
	50.5	16.5	16.0	14.0
	46.5	19.5	4.0	3.0
	59.5	83.5	5.0	5.0
	67.5	5.5	7.0	5.0
	72.5	40.5	8.0	14.0
	78.5	31.5	2.0	5.0
	105.5	4.5	7.0	4.0
	111.5	104.5	3.0	6.0
	110.5	19.5	16.0	19.0
	120.5	41.5	2.0	5.0
	118.5	16.5	10.0	16.0
	126.5	47.5	2.0	5.0
7	15.5	118.5	3.0	6.0
	23.5	62.5	15.0	12.0
	32.5	4.5	2.0	2.0
	36.5	8.5	2.0	2.0
	40.5	125.5	6.0	3.0
	40.5	96.5	2.0	2.0
	42.5	17.5	6.0	9.0
	57.5	65.5	5.0	7.0
	71.5	83.5	5.0	5.0
	71.5	125.5	5.0	3.0
	76.5	41.5	8.0	9.0
	81.5	18.5	11.0	12.0
	80.5	71.5	6.0	7.0
	80.5	9.5	2.0	3.0
	90.5	30.5	2.0	2.0
99.5	15.5	9.0	15.0	
110.5	22.5	18.0	20.0	

Table 4, cont'd.

Image No. Target(s) detected by pyramid linking

	<u>Ci</u>	<u>Cj</u>	<u>Ri</u>	<u>Rj</u>
8	2.5	11.5	2.0	5.0
	5.5	6.5	5.0	6.0
	26.5	119.5	4.0	5.0
	28.5	112.5	2.0	2.0
	29.5	11.5	9.0	11.0
	34.5	34.5	4.0	4.0
	42.5	5.5	2.0	5.0
	49.5	22.5	9.0	12.0
	105.5	10.5	3.0	4.0
	99.5	44.5	15.0	18.0
	103.5	115.5	13.0	13.0
	117.5	23.5	7.0	11.0
	112.5	18.5	16.0	18.0
	120.5	26.5	6.0	6.0
	113.5	111.5	15.0	17.0
9	2.5	120.5	2.0	2.0
	2.5	126.5	2.0	2.0
	4.5	16.5	2.0	2.0
	5.5	39.5	3.0	3.0
	9.5	2.5	3.0	2.0
	9.5	12.5	9.0	12.0
	40.5	92.5	4.0	4.0
	75.5	92.5	7.0	8.0
	76.5	102.5	2.0	2.0
	80.5	103.5	2.0	3.0
	90.5	16.5	10.0	8.0
	85.5	35.5	5.0	5.0
	91.5	66.5	3.0	4.0
	108.5	76.5	2.0	2.0
	112.5	16.5	16.0	16.0
	113.5	122.5	3.0	4.0
	107.5	118.5	9.0	10.0
	122.5	71.5	2.0	3.0
126.5	72.5	2.0	4.0	
119.5	76.5	9.0	6.0	
118.5	106.5	10.0	22.0	
10	5.5	15.5	5.0	7.0
	13.5	110.5	13.0	18.0
	30.5	101.5	2.0	5.0
	29.5	76.5	7.0	8.0
	41.5	82.5	3.0	2.0
	41.5	97.5	5.0	3.0
	53.5	122.5	3.0	4.0
	56.5	18.5	2.0	4.0
	55.5	117.5	3.0	3.0
	59.5	2.5	3.0	2.0

Table 4, cont'd.

Image No. Target(s) detected by pyramid linking

	<u>Ci</u>	<u>Cj</u>	<u>Ri</u>	<u>Rj</u>
10	52.5	30.5	10.0	16.0
	63.5	47.5	3.0	3.0
	55.5	110.5	11.0	14.0
	58.5	9.5	6.0	9.0
	70.5	80.5	2.0	2.0
	84.5	53.5	18.0	13.0
	96.5	110.5	2.0	2.0
	115.5	117.5	13.0	11.0
11	5.0	58.0	2.5	4.5
	14.5	55.5	4.0	3.0
	18.5	47.5	5.0	6.0
	19.5	44.5	3.0	2.0
	17.5	59.0	6.0	5.5
	45.5	3.0	3.0	2.5
	53.5	7.0	4.0	4.5
	54.0	3.0	2.5	2.5
	49.0	59.0	10.5	5.5
	57.5	28.5	6.0	3.0
	59.5	59.0	5.0	5.5
	58.5	13.0	6.0	12.5
	61.0	53.5	3.5	2.0
	61.0	23.0	3.5	4.5
12	36.5	36.0	5.0	12.5
13	40.5	37.5	6.0	11.0
14	7.5	48.0	2.0	2.5
	8.5	62.5	2.0	2.0
	10.0	16.0	2.5	3.5
	10.0	38.0	7.5	6.5
	19.0	48.5	6.5	4.0
	22.0	16.0	3.5	5.5
	27.5	15.0	2.0	2.5
	26.5	53.5	3.0	2.0
	33.0	36.0	11.5	17.5
	27.0	35.0	17.5	19.5
	62.5	15.5	2.0	2.0
15	30.0	41.0	12.5	20.5
16	7.0	50.5	2.5	3.0
	15.5	32.0	4.0	9.5
	13.0	7.0	6.5	6.5
	30.5	42.0	3.0	7.5

Table 4, cont'd.

Image No. Target(s) detected by pyramid linking

	<u>Ci</u>	<u>Cj</u>	<u>Ri</u>	<u>Rj</u>
16	23.0	47.0	13.5	17.5
	32.5	12.0	11.0	9.5
	41.0	7.5	2.5	2.0
	51.0	27.5	2.5	6.0
17	24.5	33.0	13.0	17.5
	34.5	32.0	15.0	18.5
	44.0	25.0	9.5	12.5
18	9.5	45.5	9.0	19.0
	26.0	57.5	2.5	2.0
	33.5	34.0	16.0	17.5
	39.0	36.0	18.5	18.5
	46.0	52.5	10.5	6.0
19	28.0	45.5	11.5	7.0
	26.0	34.0	4.5	2.5
	33.5	26.5	3.0	5.0
	37.0	35.0	17.5	18.5
	45.5	15.0	3.0	2.5
	49.0	36.0	8.5	18.5
20	34.5	49.0	16.0	14.5
	46.5	54.0	6.0	10.5
21	24.5	49.5	3.0	2.0
	34.0	54.5	4.5	3.0
	31.0	39.5	15.5	16.0
	37.5	35.0	17.0	18.5
22	2.5	20.0	2.0	2.5
	7.5	10.0	4.0	9.5
	16.0	43.5	4.5	3.0
	13.5	18.5	2.0	3.0
	13.5	55.5	2.0	2.0
	15.5	9.5	3.0	4.0
	26.0	3.0	3.5	2.5
	26.5	58.0	3.0	4.5
	26.0	11.5	3.5	4.0
	28.5	37.5	4.0	8.0
	31.0	62.0	3.5	2.5
	39.0	61.0	3.5	3.5
	46.0	32.0	14.5	12.5
	46.0	32.5	17.5	17.0
	50.0	49.0	14.5	15.5
	46.0	17.5	18.5	14.0

Table 4, cont'd.

<u>Image No.</u>	<u>Target(s) detected by pyramid linking</u>			
	<u>Ci</u>	<u>Cj</u>	<u>Ri</u>	<u>Rj</u>
23	5.0	10.0	2.5	2.5
	12.0	3.0	4.5	2.5
	17.5	49.5	4.0	5.0
	17.0	51.0	2.5	2.5
	28.0	34.0	13.5	22.5
	37.0	55.0	3.5	2.5
	27.0	19.0	15.5	18.5
	34.5	47.0	11.0	17.5
	37.5	11.5	10.0	11.0
	59.5	10.0	5.0	9.5
24	22.0	49.5	2.5	4.0
	32.5	43.5	3.0	2.0
	36.5	40.0	13.0	20.5
	46.0	62.0	3.5	2.5
	55.5	18.0	3.0	2.5
	57.0	60.5	3.5	4.0
	58.0	24.0	2.5	2.5
25	41.5	42.5	10.0	11.0
26	3.0	23.0	2.5	3.5
	26.0	36.0	8.5	12.5
	28.5	31.5	9.0	11.0
	54.5	45.5	3.0	7.0
	56.5	36.0	2.0	2.5
	54.0	11.5	4.5	5.0
27	14.5	49.5	5.0	7.0
	20.5	25.0	5.0	8.5
	27.5	24.0	3.0	3.5
	28.5	24.5	11.0	9.0
	35.5	24.5	8.0	12.0
28	6.0	24.5	4.5	6.0
	6.5	8.0	4.0	7.5
	28.5	25.5	12.0	11.0
	32.5	45.0	2.0	2.5
	45.5	20.0	2.0	2.5
	49.0	12.5	4.5	4.0
	50.0	25.5	3.5	4.0
	49.5	4.5	5.0	4.0
	58.0	10.0	2.5	3.5

Table 4, cont'd.

Image No. Target(s) detected by pyramid linking

	<u>Ci</u>	<u>Cj</u>	<u>Ri</u>	<u>Rj</u>
29	15.0	7.0	4.5	6.5
	29.0	10.5	3.5	6.0
	29.0	42.5	13.5	11.0
	40.5	25.0	4.0	2.5
	44.0	4.5	5.5	4.0
	48.0	6.0	2.5	2.5
	57.5	28.5	2.0	3.0
	55.0	9.5	9.5	7.0
30	19.5	28.0	5.0	2.5
	34.5	44.0	5.0	3.5
	43.5	23.5	2.0	2.0
	47.0	41.0	15.5	13.5
	53.0	26.0	11.5	7.5
	58.5	42.0	6.0	9.5
31	6.5	3.5	2.0	3.0
	28.5	119.5	16.0	9.0
	66.5	126.5	2.0	2.0
	98.5	15.5	8.0	15.0
	115.5	38.5	5.0	8.0
	117.5	4.5	5.0	4.0
	123.5	125.5	5.0	3.0
32	8.5	2.5	2.0	2.0
	57.5	70.5	11.0	12.0
	70.5	125.5	6.0	3.0
	106.5	11.5	4.0	5.0
	110.5	23.5	2.0	5.0
	114.5	37.5	4.0	9.0
	120.5	15.5	8.0	15.0
33	8.5	50.5	8.0	16.0
	4.5	58.5	4.0	8.0
	41.5	103.5	5.0	3.0
	46.5	37.5	2.0	3.0
	49.5	65.5	3.0	3.0
	53.5	87.5	5.0	7.0
	52.5	106.5	2.0	4.0
	53.5	113.5	3.0	5.0
	54.5	103.5	2.0	3.0
	51.5	58.5	11.0	12.0
	54.5	76.5	8.0	10.0
	60.5	88.5	2.0	2.0
	63.5	94.5	5.0	4.0
	65.5	48.5	9.0	20.0
	66.5	78.5	2.0	2.0
65.5	90.5	3.0	4.0	

Table 4, cont'd.

Image No. Target(s) detected by pyramid linking

	<u>Ci</u>	<u>Cj</u>	<u>Ri</u>	<u>Rj</u>
33	71.5	58.5	9.0	16.0
	75.5	68.5	9.0	14.0
	78.5	46.5	2.0	2.0
	86.5	84.5	10.0	6.0
	79.5	108.5	13.0	20.0
	111.5	86.5	11.0	8.0
34	2.5	2.5	2.0	2.0
	4.5	103.5	4.0	7.0
	14.5	84.5	2.0	4.0
	28.5	21.5	4.0	5.0
	40.5	124.5	4.0	4.0
	37.5	3.5	5.0	3.0
	41.5	90.5	3.0	2.0
	43.5	14.5	3.0	4.0
	44.5	117.5	4.0	3.0
	42.5	108.5	6.0	6.0
	48.5	97.5	6.0	15.0
	51.5	80.5	5.0	6.0
	53.5	124.5	7.0	4.0
	67.5	76.5	3.0	4.0
	62.5	69.5	12.0	13.0
	73.5	90.5	3.0	4.0
	70.5	117.5	6.0	11.0
	86.5	70.5	2.0	4.0
	90.5	64.5	2.0	2.0
	113.5	11.5	11.0	11.0
	102.5	75.5	10.0	15.0
	113.5	97.5	5.0	7.0
	112.5	126.5	2.0	2.0
	116.5	70.5	4.0	4.0
110.5	116.5	8.0	12.0	
115.5	76.5	3.0	2.0	
118.5	89.5	4.0	3.0	
121.5	115.5	7.0	13.0	
117.5	38.5	7.0	16.0	
124.5	15.5	2.0	3.0	
35	3.5	90.5	3.0	4.0
	2.5	101.5	2.0	3.0
	8.5	82.5	4.0	6.0
	9.5	14.5	9.0	12.0
	25.5	5.5	7.0	5.0
	19.5	13.5	3.0	3.0
	11.5	108.5	11.0	20.0
	23.5	77.5	3.0	3.0
	22.5	51.5	2.0	3.0
	18.5	95.5	10.0	9.0
	28.5	104.5	4.0	2.0
	21.5	118.5	7.0	10.0

Table 4, cont'd.

Image No. Target(s) detected by pyramid linking

	<u>Ci</u>	<u>Cj</u>	<u>Ri</u>	<u>Rj</u>
35	23.5	82.5	5.0	8.0
	30.5	45.5	2.0	3.0
	28.5	82.5	2.0	4.0
	29.5	98.5	3.0	4.0
	31.5	60.5	7.0	12.0
	38.5	44.5	4.0	2.0
	34.5	7.5	6.0	5.0
	41.5	111.5	7.0	15.0
	38.5	90.5	4.0	6.0
	44.5	32.5	4.0	4.0
	42.5	111.5	10.0	17.0
	49.5	14.5	3.0	4.0
	53.5	20.5	3.0	4.0
	63.5	23.5	3.0	3.0
	76.5	81.5	2.0	3.0
	80.5	77.5	2.0	3.0
36	8.5	116.5	4.0	4.0
	9.5	42.5	3.0	4.0
	18.5	69.5	2.0	3.0
	18.5	25.5	6.0	7.0
	22.5	89.5	2.0	3.0
	13.5	113.5	13.0	15.0
	25.5	14.5	7.0	6.0
	44.5	102.5	4.0	6.0
	65.6	113.5	17.0	15.0
	68.5	71.5	14.0	13.0
	111.5	20.5	17.0	20.0
	55	48.5	125.5	2.0
75.5		125.5	3.0	3.0
102.5		36.5	2.0	2.0
56	-	-	-	-
57	22.5	95.5	2.0	5.0
	29.5	100.5	3.0	6.0
	25.5	122.5	3.0	6.0
	34.5	10.5	4.0	8.0
	35.5	106.5	3.0	6.0
	35.5	123.5	3.0	5.0
	60.5	108.5	2.0	2.0
	60.5	117.5	2.0	3.0

Table 4, cont'd.

<u>Image No.</u>	<u>Target(s) detected by pyramid linking</u>			
	<u>Ci</u>	<u>Cj</u>	<u>Ri</u>	<u>Rj</u>
58	26.5	22.5	2.0	4.0
	23.5	16.5	9.0	14.0
59	-	-	-	-
60	32.5	24.5	10.0	22.0
	74.5	115.5	2.0	3.0
	89.5	102.5	5.0	10.0
61	77.5	75.5	7.0	11.0
62	73.5	56.5	3.0	2.0
	94.5	99.5	8.0	15.0
63	96.5	39.5	2.0	3.0
64	28.5	5.5	2.0	3.0
65	14.5	126.5	2.0	2.0
	80.5	100.5	2.0	2.0
	78.5	115.5	8.0	13.0
66	85.5	115.5	11.0	13.0
	116.5	122.5	4.0	6.0
67	85.5	117.5	5.0	11.0
68	84.5	123.5	2.0	5.0
	107.5	113.5	13.0	15.0
69	17.5	125.5	3.0	3.0
	69.5	126.5	3.0	2.0
	80.5	55.5	4.0	9.0
	104.5	7.5	10.0	7.0
	104.5	17.5	4.0	5.0
70	31.5	57.5	7.0	5.0
	37.5	46.5	3.0	4.0
	47.5	79.5	3.0	3.0
	51.5	104.5	3.0	2.0
	75.5	69.5	3.0	5.0
	83.5	2.5	3.0	2.0
	86.5	34.5	2.0	4.0
	114.5	113.5	2.0	3.0
	106.5	118.5	14.0	10.0

Table 4, cont'd.

Image No. Target(s) detected by superspike

	<u>Ci</u>	<u>Cj</u>	<u>Ri</u>	<u>Rj</u>
2	16.5	6.5	4.0	4.0
	17.5	93.0	7.0	4.5
	52.5	121.5	10.0	5.0
	51.5	94.0	5.0	5.5
	57.5	38.0	15.0	14.5
	96.5	15.0	4.0	6.5
	91.5	47.0	13.0	14.5
	108.5	98.5	2.0	2.0
	109.5	119.0	7.0	6.5
	111.5	108.0	5.0	7.5
	3	8.0	69.5	5.5
19.5		17.0	2.0	4.5
43.0		91.5	2.5	3.0
59.5		47.5	10.0	9.0
68.0		115.5	9.5	11.0
77.5		14.0	12.0	11.5
104.5		106.0	9.0	15.5
4		112.0	3.5	6.5
	3.0	4.5	116.5	2.0
	3.0	7.5	2.5	5.0
	17.5	4.5	5.0	6.0
	3.5	3.5	108.0	12.0
	18.5	24.0	2.0	3.5
	26.0	3.5	3.5	10.0
	9.0	7.5	11.5	8.5
	5.0	38.5	5.0	4.0
	20.0	3.0	4.5	37.5

Target 5. Targets detected by superspike
in each image.

Image No. Target(s) detected by superspike

	<u>Ci</u>	<u>Cj</u>	<u>Ri</u>	<u>Rj</u>
5	34.0	48.0	4.5	4.5
	99.0	39.5	2.5	5.0
	98.5	107.0	2.0	4.5
	111.5	28.5	4.0	6.0
6	51.5	18.0	15.0	15.5
	73.0	40.5	7.5	15.0
	117.0	6.0	3.5	3.5
	110.5	19.0	16.0	16.5
	119.5	18.5	7.0	11.0
7	8.0	94.0	2.5	4.5
	27.0	93.0	2.5	2.5
	30.0	52.0	2.5	2.5
	51.5	80.5	4.0	7.0
	67.0	56.5	2.5	3.0
	80.5	34.0	2.0	2.5
	88.5	46.0	5.0	12.5
	90.5	9.5	5.0	7.0
	111.5	93.0	5.0	7.5
8	5.0	10.5	2.5	6.0
	24.0	43.0	2.5	3.5
	24.0	53.5	2.5	6.0
	31.5	7.5	6.0	5.0
	72.5	36.5	7.0	7.0
	75.5	60.0	4.0	8.5
	80.5	80.5	3.0	5.0
	83.5	111.5	8.0	15.0
	98.5	45.5	3.0	2.0
	114.0	29.5	2.5	5.0
	117.5	4.5	2.0	2.0
9	15.5	113.0	2.0	2.5
	20.5	124.5	4.0	2.0
	21.5	111.5	2.0	2.0
	20.5	114.0	3.0	2.5
	32.0	116.0	5.5	6.5
	41.5	91.5	2.0	2.0
	85.5	13.0	2.0	2.5
	89.5	17.5	4.0	4.0
	88.5	35.0	3.0	3.5
	94.5	18.5	3.0	3.0
	101.5	4.5	2.0	2.0
	108.0	52.5	3.5	4.0

Table 5, cont'd.

Image No. Target(s) detected by superspike

	<u>Ci</u>	<u>Cj</u>	<u>Ri</u>	<u>Rj</u>
9	109.5	22.0	2.0	3.5
	120.5	16.5	3.0	5.0
	124.0	4.5	2.5	2.0
	114.0	24.5	12.5	22.0
	113.0	44.0	13.5	19.5
10	17.0	120.5	5.5	6.0
	29.5	74.0	7.0	8.5
	48.5	41.0	3.0	3.5
	93.5	53.5	2.0	3.0
	118.0	63.0	2.5	3.5
	118.5	76.0	3.0	5.5
	117.5	101.5	9.0	10.0
11	56.5	19.5	2.0	5.0
	54.0	53.5	7.5	8.0
12	36.5	35.5	6.0	12.0
	35.5	39.0	2.0	3.5
	54.0	56.0	7.5	5.5
	51.0	30.0	2.5	2.5
	57.0	33.5	4.5	7.0
13	41.5	43.5	3.0	2.0
	40.5	37.0	6.0	11.5
14	31.5	36.0	14.0	18.5
15	29.0	39.5	13.5	20.0
16	31.0	42.5	2.5	5.0
17	32.5	31.5	19.0	19.0
18	39.5	36.0	19.0	19.5
19	37.5	35.0	19.0	19.5
20	15.5	55.0	2.0	2.5
	28.5	27.0	8.0	14.5
	21.0	45.0	3.5	5.5
	39.0	33.5	2.5	2.0
	33.5	47.5	17.0	14.0
21	32.0	39.0	15.5	16.5
	44.5	24.5	2.0	2.0

Table 5, cont'd.

<u>Image No.</u>	<u>Target(s) detected by superspike</u>			
	<u>Ci</u>	<u>Cj</u>	<u>Ri</u>	<u>Rj</u>
22	46.0	32.5	15.5	15.0
23	28.0	34.0	13.5	22.5
24	37.5	40.0	12.0	20.5
25	10.5	40.5	2.0	3.0
	20.5	10.5	2.0	3.0
	42.0	43.0	9.5	11.5
26	26.0	36.5	8.5	12.0
27	28.5	24.5	12.0	11.0
28	23.5	32.5	4.0	3.0
	29.0	25.5	11.5	11.0
29	20.0	45.5	3.5	3.0
	18.0	36.5	2.5	3.0
	29.5	47.5	2.0	4.0
	28.0	41.5	11.5	9.0
	38.0	42.0	4.5	10.5
30	43.0	42.0	3.5	5.5
	52.5	46.5	2.0	2.0
	44.5	39.5	12.0	12.0
31	21.5	123.5	5.0	3.0
	61.0	74.5	6.5	12.0
	114.0	38.0	2.5	3.5
32	23.0	111.5	20.5	15.0
	60.5	70.0	6.0	9.5
	124.5	17.5	2.0	5.0
33	5.5	42.5	3.0	4.0
	13.0	19.0	8.5	16.5
	27.5	55.5	2.0	3.0
	31.0	81.5	3.5	7.0
	32.0	63.5	5.5	5.0
	35.0	89.0	2.5	4.5
	41.0	84.0	8.5	11.5
	42.5	95.5	6.0	5.0
	42.5	75.5	5.0	9.0
50.5	92.0	5.0	8.5	

Table 5, cont'd.

Image No. Target(s) detected by superspike

	<u>Ci</u>	<u>Cj</u>	<u>Ri</u>	<u>Rj</u>
33	55.5	111.0	3.0	4.5
	55.0	98.0	5.5	9.5
	59.0	110.5	2.5	5.0
	64.5	116.5	6.0	9.0
	71.5	60.5	15.0	22.0
	98.0	109.0	16.5	17.5
	117.0	99.5	6.5	6.0
	121.0	97.0	2.5	3.5
	124.0	114.0	2.5	4.5
34	6.5	33.0	4.0	5.5
	13.0	21.0	2.5	2.5
	14.5	83.5	3.0	4.0
	33.5	44.0	3.0	2.5
	66.5	78.0	2.0	3.5
	68.0	75.5	2.5	3.0
35	6.5	80.5	2.0	3.0
	6.5	83.0	4.0	7.5
	11.5	15.0	2.0	4.5
	10.0	12.5	7.5	10.0
	17.5	62.5	2.0	2.0
	15.5	67.0	3.0	5.5
	20.5	4.5	3.0	2.0
	20.5	104.0	2.0	2.5
	18.0	89.0	9.5	15.5
	25.5	79.5	3.0	3.0
	22.5	85.5	4.0	6.0
	26.5	94.5	2.0	3.0
	30.5	58.5	5.0	3.0
	29.0	100.0	3.5	5.5
	29.5	70.5	3.0	3.0
	30.5	7.5	2.0	2.0
	30.5	43.5	2.0	2.0
	27.5	84.0	3.0	7.5
	36.5	45.0	5.0	3.5
	35.5	120.5	2.0	2.0
	36.5	9.0	2.0	2.5
	34.5	55.5	5.0	7.0
	39.5	123.5	2.0	3.0
	43.5	76.0	7.0	7.5
	43.0	91.0	7.5	6.5
	41.5	111.5	8.0	15.0
44.0	33.0	2.5	4.5	
54.0	48.5	2.5	2.0	
55.5	51.0	2.0	3.5	
53.5	66.0	14.0	15.5	

Table 5, cont'd.

Image No. Target(s) detected by superspike

	<u>Ci</u>	<u>Cj</u>	<u>Ri</u>	<u>Rj</u>
35	56.5	78.0	2.0	2.5
	63.0	23.0	3.5	3.5
	61.5	110.0	2.0	3.5
	67.5	11.5	2.0	2.0
	68.5	62.0	6.0	5.5
	77.5	7.0	2.0	4.5
	84.5	11.0	7.0	8.5
36	19.5	20.5	17.0	18.0
	34.5	90.0	3.0	3.5
	42.5	6.0	6.0	3.5
	68.5	72.5	15.0	12.0
	62.5	113.0	15.0	13.5
	106.0	25.5	20.5	23.0
55	84.0	81.0	3.5	6.5
	85.0	106.5	2.5	4.0
56	84.0	78.0	3.5	7.5
	85.0	106.5	2.5	4.0
57	91.0	74.5	3.5	8.0
	93.5	106.5	3.0	5.0
58	102.0	72.5	4.5	9.0
	103.5	108.0	3.0	5.5
59	99.0	111.0	3.5	6.5
60	62.5	24.5	3.0	6.0
	86.5	52.5	6.0	13.0
	89.5	103.5	4.0	8.0
61	77.0	16.0	7.5	13.5
	78.0	75.5	5.5	11.0
62	91.5	19.5	11.0	17.0
	95.0	99.0	7.5	14.5
63	85.0	6.0	2.5	3.5
64	-	-	-	-
65	94.5	9.5	3.0	7.0
	95.5	33.5	2.0	2.5

Table 5, cont'd.

<u>Image No.</u>	<u>Target(s) detected by superspike</u>			
	<u>Ci</u>	<u>Cj</u>	<u>Ri</u>	<u>Rj</u>
66	103.5	20.0	3.0	2.5
	104.5	11.5	2.0	4.0
67	100.0	23.0	3.5	8.5
	101.5	53.5	2.0	4.0
68	90.0	24.0	4.5	10.5
	92.0	61.0	2.5	5.5
69	78.0	13.0	5.5	10.5
	79.5	59.0	3.0	4.5
70	93.5	62.0	2.0	2.5
	96.5	55.5	8.0	19.0

Table 5, cont'd.

<u>Image No.</u>	<u>True targets</u>	<u>Correctly detected</u>	<u>Extra detections</u>	<u>False alarms</u>	<u>Segmentation accuracy</u>
2	3	0	0	3	
3	2	0	0	1	
4	0	0	0	4	
5	0	0	0	6	
6	0	0	0	0	
7	0	0	0	6	
8	2	0	0	1	
9	1	0	0	15	
10	0	0	0	7	
11	4	0	0	8	
12	4	0	0	4	
13	4	0	0	8	
14	4	4	0	0	0.654
15	4	4	0	0	0.675
16	4	4	0	16	0.818
17	4	0	0	0	
18	4	0	0	8	
19	4	0	0	0	
20	4	0	0	0	
21	4	4	0	0	0.920
22	4	4	0	0	0.845
23	4	0	0	4	
24	4	4	0	0	0.759
25	4	0	0	0	
26	4	4	0	4	0.806
27	4	4	0	4	0.830
28	4	4	0	20	0.447
29	4	4	0	8	0.547
30	4	0	0	8	

Table 6. Performance of 2-class relaxation for each image.

<u>Image No.</u>	<u>True targets</u>	<u>Correctly detected</u>	<u>Extra detections</u>	<u>False alarms</u>	<u>Segmentation accuracy</u>
31	1	1	0	2	0.691
32	1	0	0	3	
33	1	1	0	0	0.787
34	1	0	0	1	
35	1	0	0	3	
36	1	0	0	0	
55	2	0	0	0	
56	2	0	0	0	
57	2	0	0	0	
58	2	0	0	0	
59	2	0	0	0	
60	2	0	0	1	
61	2	1	0	2	0.593
62	2	1	0	1	0.748
63	2	0	0	0	
64	2	0	0	0	
65	2	0	0	0	
66	2	0	0	1	
67	2	0	0	0	
68	2	0	0	0	
69	2	0	0	0	
70	2	0	0	1	

Table 6, cont'd.

<u>Image No.</u>	<u>True targets</u>	<u>Correctly detected</u>	<u>Extra detections</u>	<u>False alarms</u>	<u>Segmentation accuracy</u>
2	3	1	0	8	0.682
3	2	0	0	6	
4	0	0	0	8	
5	0	0	0	5	
6	0	0	0	1	
7	0	0	0	10	
8	2	0	0	10	
9	1	1	0	9	0.711
10	0	0	0	8	
11	4	0	0	12	
12	4	4	0	4	0.200
13	4	0	0	8	
14	4	4	8	0	0.081
15	4	0	0	0	
16	4	0	0	24	
17	4	0	0	0	
18	4	0	0	12	
19	4	0	0	0	
20	4	0	0	0	
21	4	4	0	0	0.651
22	4	0	0	16	
23	4	0	0	8	
24	4	0	0	0	
25	4	0	0	0	
26	4	0	0	4	
27	4	4	0	0	0.681
28	4	4	0	0	0.845
29	4	0	0	0	
30	4	0	0	4	

Table 7. Performance of 3-class relaxation for each image.

<u>Image No.</u>	<u>True targets</u>	<u>Correctly detected</u>	<u>Extra detections</u>	<u>False alarms</u>	<u>Segmentation accuracy</u>
31	1	1	0	7	0.917
32	1	1	0	5	0.719
33	1	1	1	10	0.571
34	1	0	0	1	
35	1	0	0	3	
36	1	0	0	1	
55	2	0	0	0	
56	2	0	0	1	
57	2	2	0	0	0.514
58	2	2	0	1	0.648
59	2	2	0	1	0.730
60	2	2	0	1	0.813
61	2	2	0	0	0.738
62	2	2	1	2	0.734
63	2	0	0	4	
64	2	0	0	0	
65	2	0	0	0	
66	2	0	0	2	
67	2	1	0	0	0.085
68	2	0	0	1	
69	2	0	0	3	
70	2	0	0	3	

Table 7, cont'd.

<u>Image No.</u>	<u>True targets</u>	<u>Correctly detected</u>	<u>Extra detections</u>	<u>False alarms</u>	<u>Segmentation accuracy</u>
2	3	0	0	20	
3	2	0	0	15	
4	0	0	0	9	
5	0	0	0	15	
6	0	0	0	15	
7	0	0	0	17	
8	2	0	0	15	
9	1	0	0	21	
10	0	0	0	18	
11	4	0	0	56	
12	4	4	0	0	0.960
13	4	4	0	0	0.880
14	4	4	4	36	0.745
15	4	4	0	0	0.853
16	4	4	0	28	0.357
17	4	4	0	8	0.705
18	4	4	0	16	0.690
19	4	4	4	16	0.495
20	4	4	0	4	0.856
21	4	4	4	8	0.704
22	4	4	4	56	0.772
23	4	0	0	40	
24	4	4	4	20	0.429
25	4	4	0	0	0.716
26	4	4	4	16	0.712
27	4	4	8	8	0.288
28	4	4	0	32	0.673
29	4	4	0	28	0.859
30	4	4	0	20	0.431

Table 8. Performance of pyramid linking for each image.

<u>Image No.</u>	<u>True targets</u>	<u>Correctly detected</u>	<u>Extra detections</u>	<u>False alarms</u>	<u>Segmentation accuracy</u>
31	1	0	0	7	
32	1	0	0	7	
33	1	1	1	20	0.530
34	1	1	1	28	0.344
35	1	0	0	28	
36	1	1	0	10	0.841
55	2	0	0	2	
56	2	0	0	0	
57	2	0	0	8	
58	2	0	0	2	
59	2	0	0	0	
60	2	1	0	2	0.779
61	2	1	0	0	0.891
62	2	1	0	1	0.822
63	2	0	0	1	
64	2	0	0	1	
65	2	0	0	3	
66	2	0	0	2	
67	2	0	0	1	
68	2	0	0	2	
69	2	1	0	4	0.700
70	2	0	0	9	

Table 8, cont'd.

<u>Image No.</u>	<u>True targets</u>	<u>Correctly detected</u>	<u>Extra detections</u>	<u>False alarms</u>	<u>Segmentation accuracy</u>
2	3	2	0	8	0.642
3	2	0	0	7	
4	0	0	0	10	
5	0	0	0	4	
6	0	0	0	5	
7	0	0	0	9	
8	2	0	0	11	
9	1	1	0	16	0.250
10	0	0	0	7	
11	1	1	0	1	0.513
12	1	1	1	3	0.475
13	1	1	1	0	0.500
14	1	1	0	0	0.966
15	1	1	0	0	0.941
16	1	1	0	0	0.198
17	1	1	0	0	0.542
18	1	1	0	0	0.638
19	1	1	0	0	0.924
20	1	1	0	4	0.938
21	1	1	0	1	0.836
22	1	1	0	0	0.804
23	1	0	0	1	
24	1	1	0	0	0.834
25	1	1	0	2	0.713
26	1	1	0	0	0.767
27	1	1	0	0	0.555
28	1	1	1	0	0.353
29	1	1	2	2	0.253
30	1	1	1	1	0.420

Table 9. Performance of superspike for each image.

<u>Image No.</u>	<u>True targets</u>	<u>Correctly detected</u>	<u>Extra detections</u>	<u>False alarms</u>	<u>Segmentation accuracy</u>
31	1	1	0	2	0.892
32	1	1	0	2	0.543
33	1	1	0	18	0.644
34	1	1	1	4	0.029
35	1	1	0	32	0.731
36	1	1	0	5	0.788
55	2	2	0	0	0.682
56	2	2	0	0	0.900
57	2	2	0	0	1.000
58	2	2	0	0	1.000
59	2	1	0	0	0.758
60	2	2	0	1	0.835
61	2	2	0	0	0.826
62	2	2	0	0	0.840
63	2	1	0	0	0.489
64	2	0	0	0	
65	2	2	0	0	0.631
66	2	1	0	1	0.250
67	2	2	0	0	0.523
68	2	2	0	0	0.726
69	2	2	0	0	0.555
70	2	1	1	0	0.488

Table 9, cont'd.

<u>Images</u>	<u>Targets</u>	<u>Method</u>	<u>Correctly detected</u>	<u>Extra detections</u>	<u>False alarms</u>	<u>Segmentation accuracy</u>
2-10 (Navy, China Lake)	8	2-class relaxation 3-class relaxation Pyramid linking Superspike	0 2 0 3	0 0 0 0	43 67 145 77	- 0.70 - 0.51
11-30 (NVL data)	80		40 20 72 76	0 8 32 24	92 92 392 60	0.73 0.49 0.67 0.64
31-36 (Air Force, TASVAL)	6		2 3 3 6	0 1 2 1	9 27 100 63	0.74 0.73 0.57 0.60
55-70 (NVL flight test)	32		2 13 4 26	0 1 0 1	6 19 38 2	0.67 0.65 0.80 0.73
Overall	126		44 38 79 111	0 10 34 26	150 205 675 202	0.73 0.58 0.68 0.66

Table 10. Summary of results by image class.

Figures 1(a-c)

Upper picture:

Input image (upper left), superslice results (lower left),
and pyramid linking results (lower right).

Lower picture:

Results using 2-class relaxation (upper left), 3-class
relaxation (upper right), pyramid linking (lower left),
and superspike (lower right).

**Best
Available
Copy**

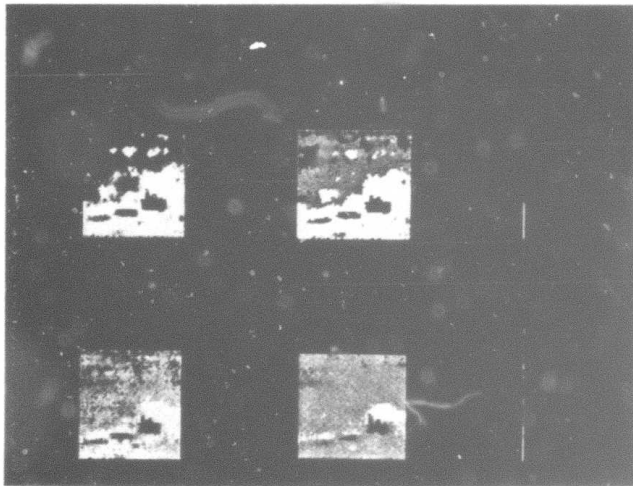
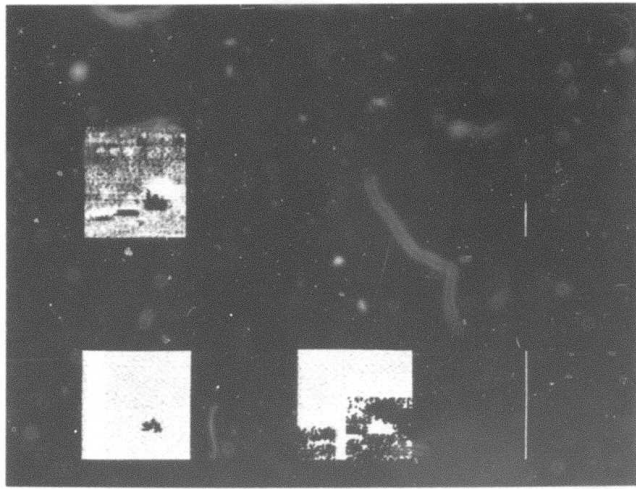


Figure 1a

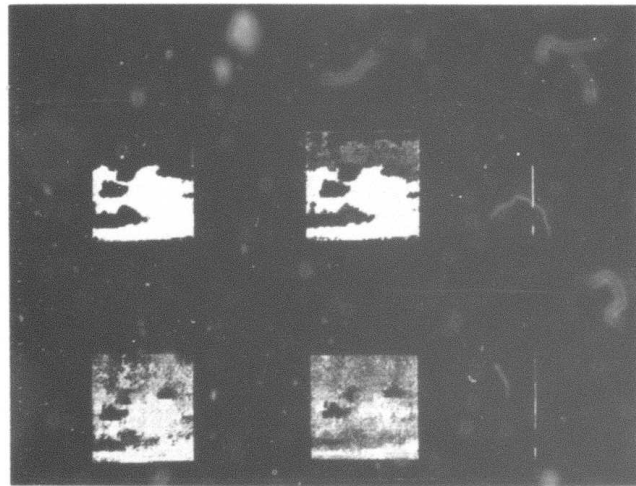
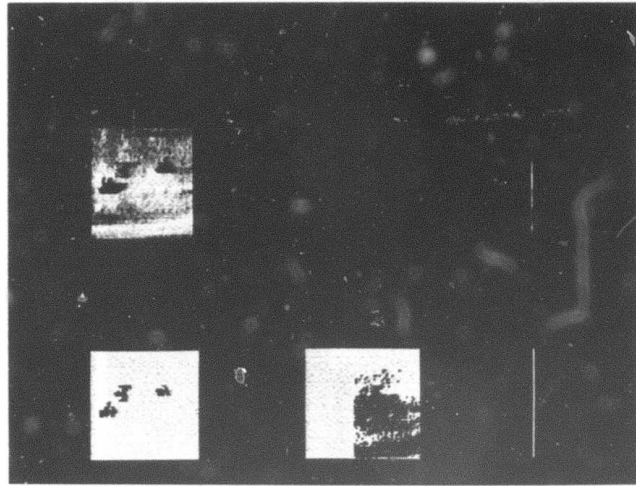


Figure 1b

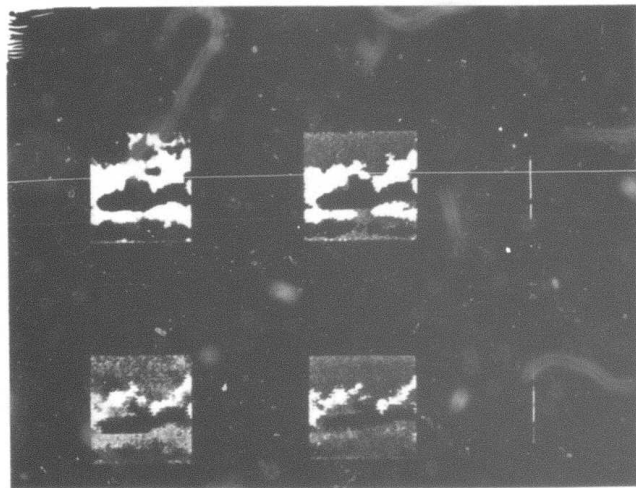
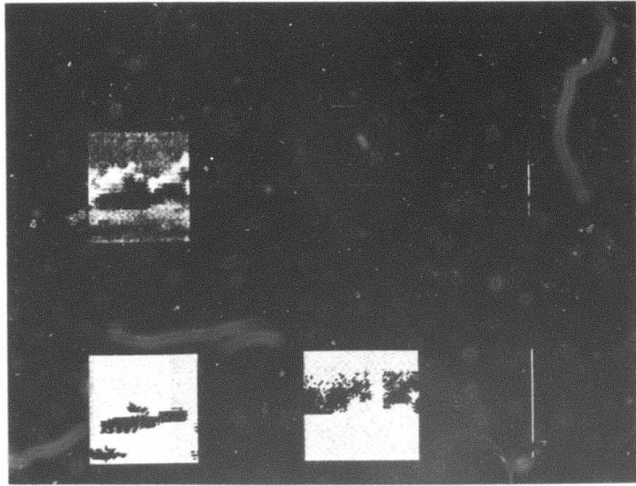
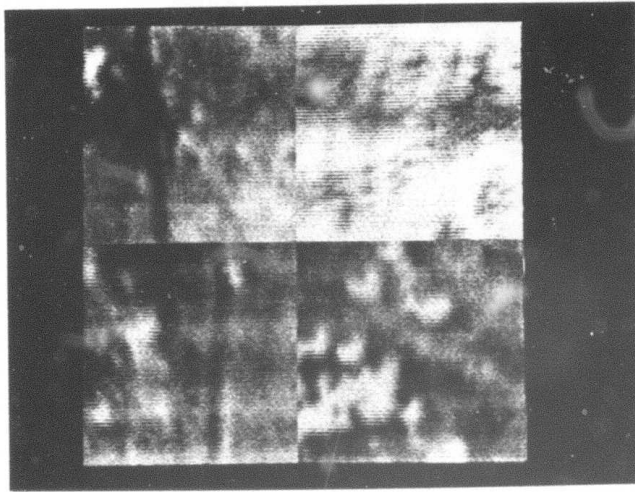
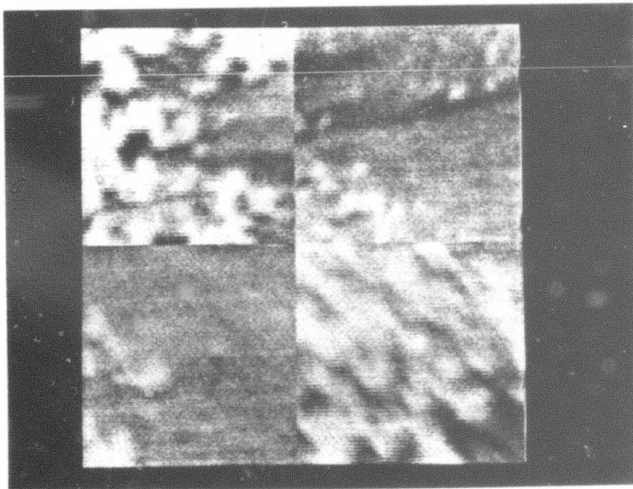


Figure 1c

Figure 2: Images
used in main study

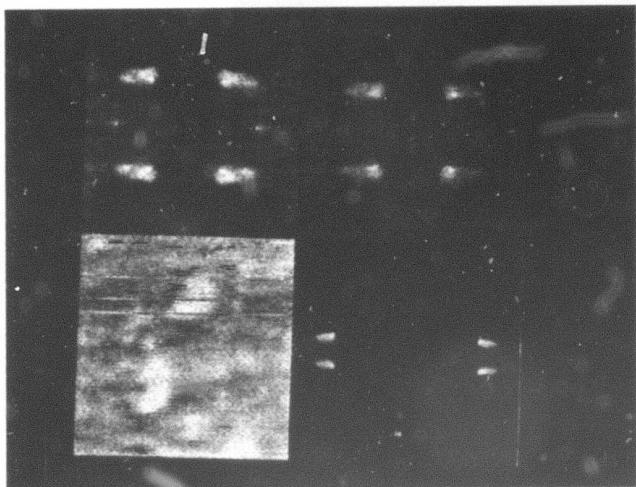


4 5
2 3



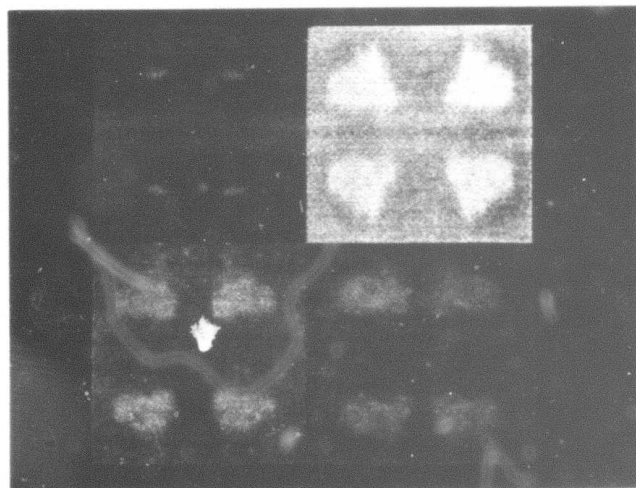
8 9
6 7

Figure 2



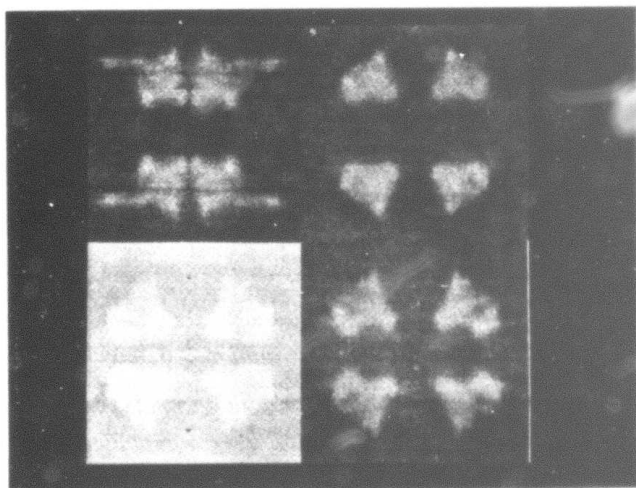
12 13

10 11



16 17

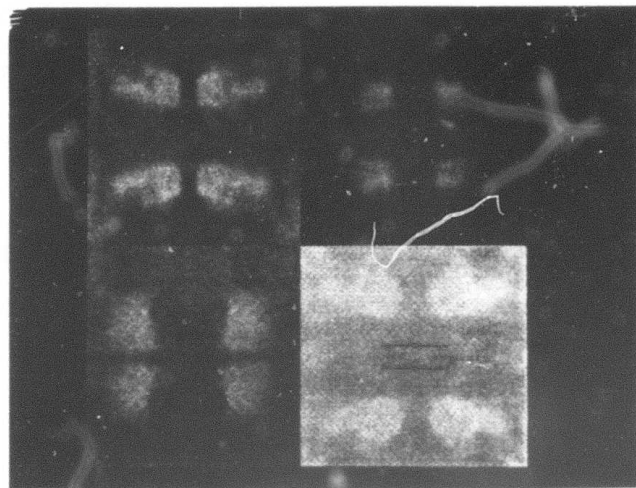
14 15



20 21

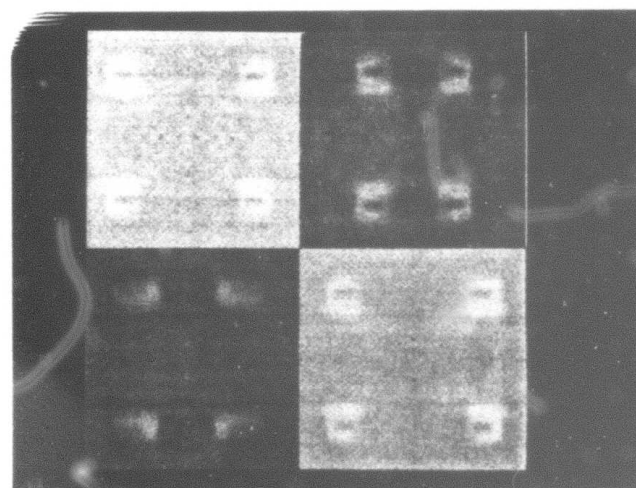
18 19

Figure 2



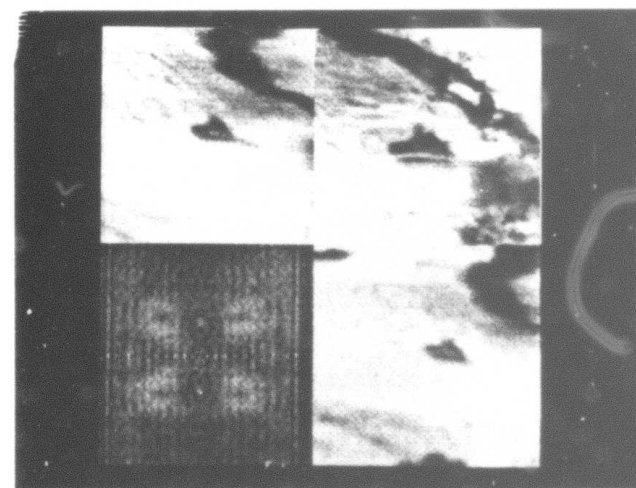
24 25

22 23



28 29

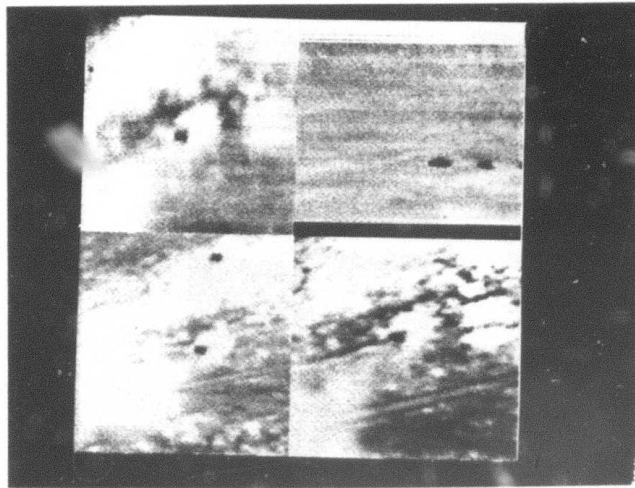
26 27



32 33

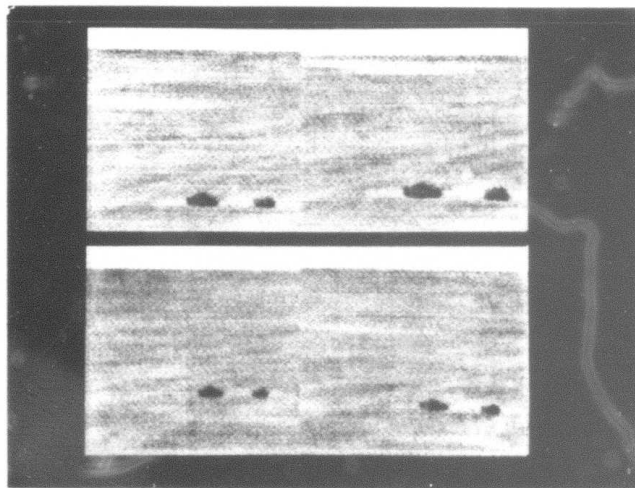
30 31

Figure 2



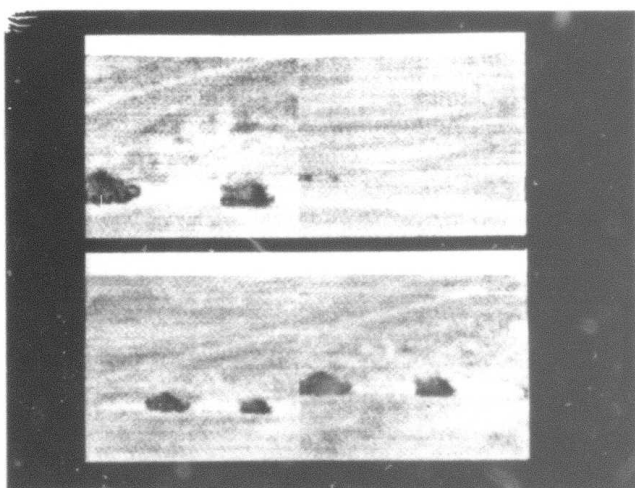
36 55

34 35



58 59

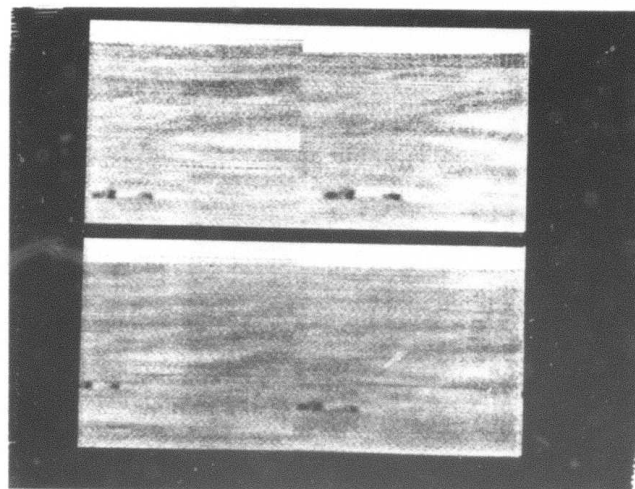
56 57



62 63

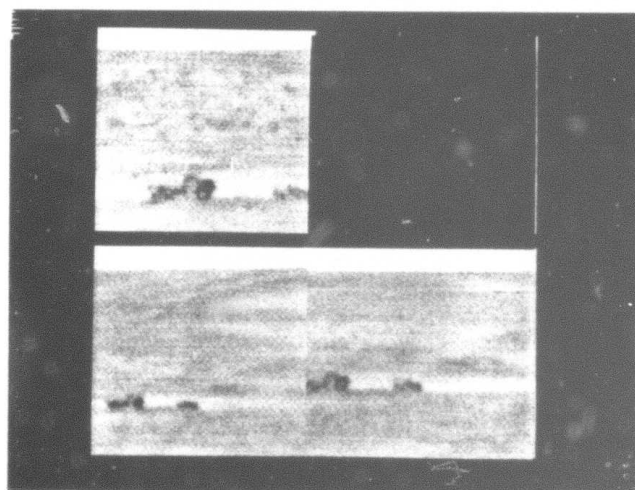
60 61

Figure 2



66 67

64 65



70

68 69

Figure 3: Results of main study.

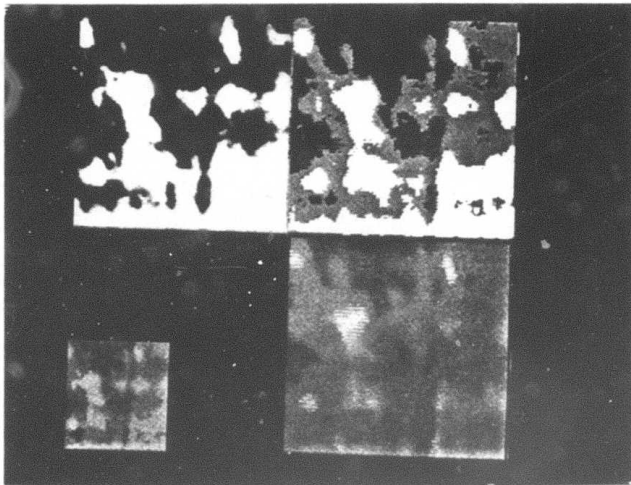
Upper left: 2-class relaxation

Upper right: 3-class relaxation

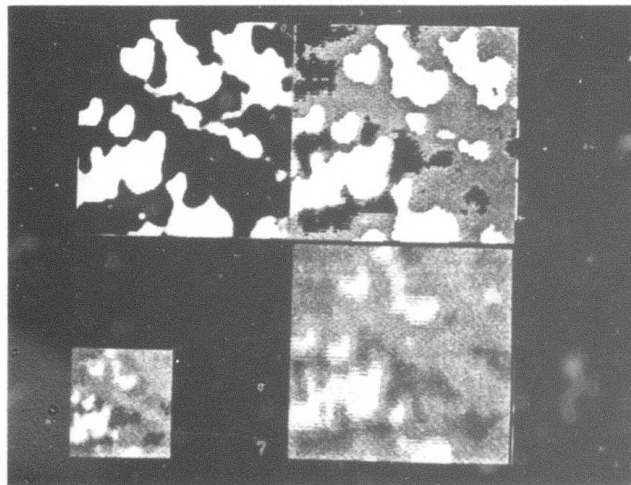
Lower left: Pyramid linking

Lower right: Superspike

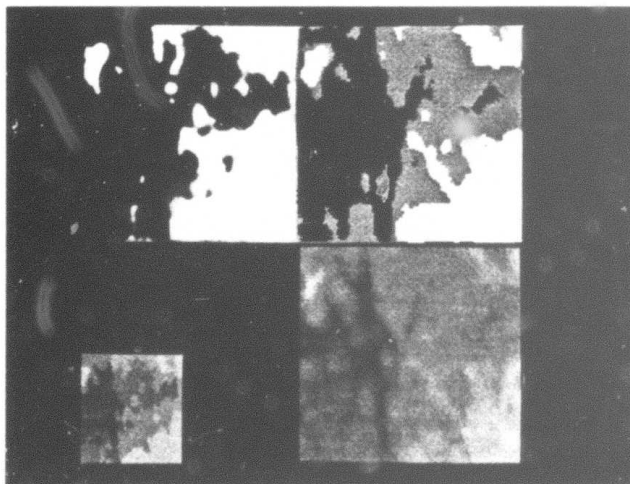
Figure 3:



2

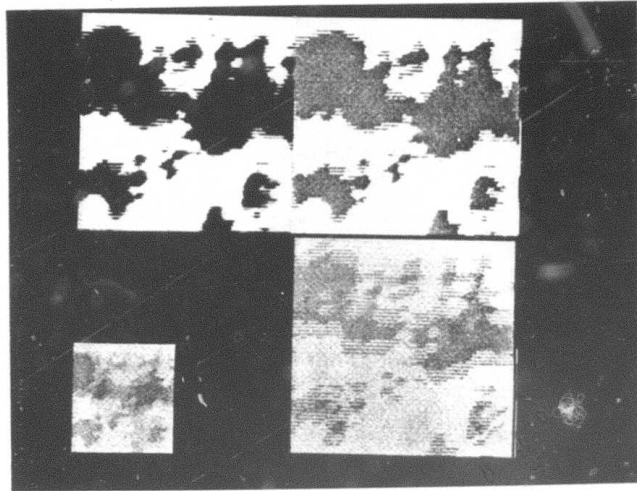


3

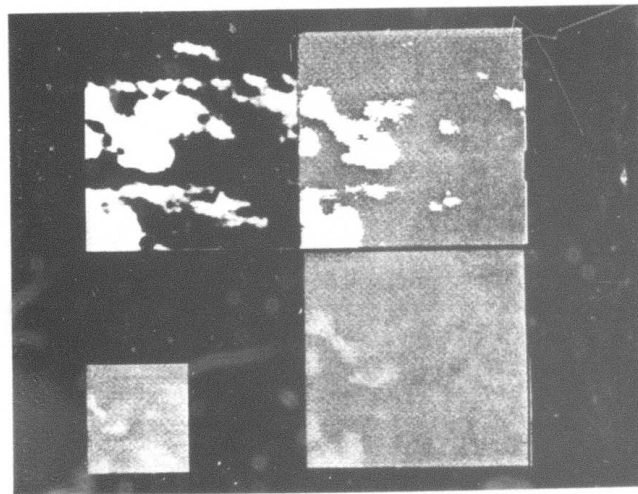


4

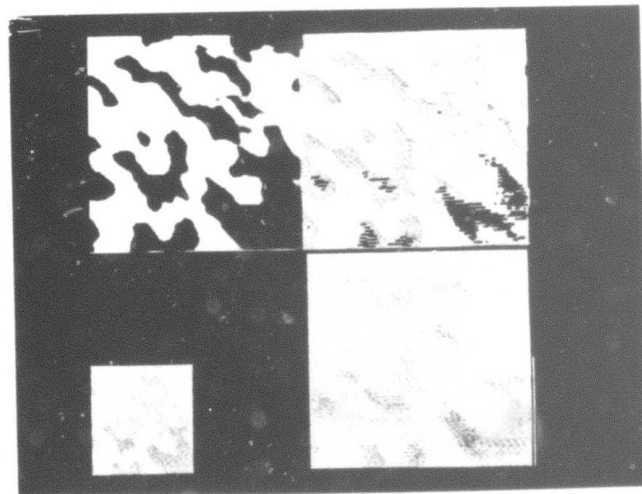
Figure 3:



5

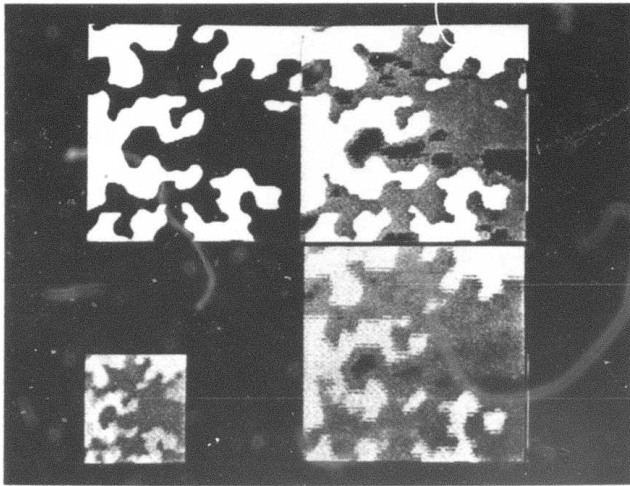


6

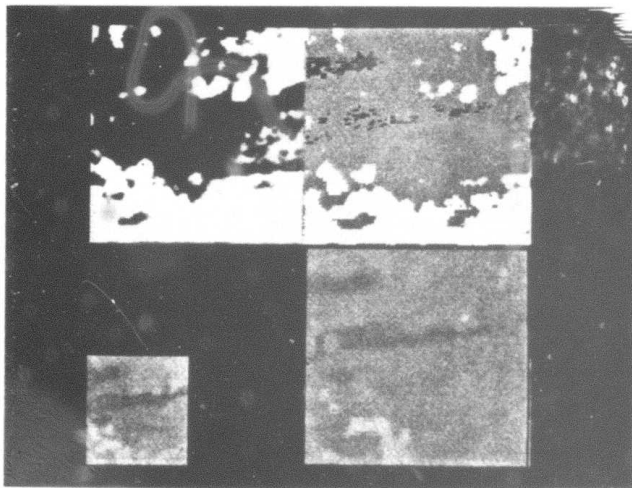


7

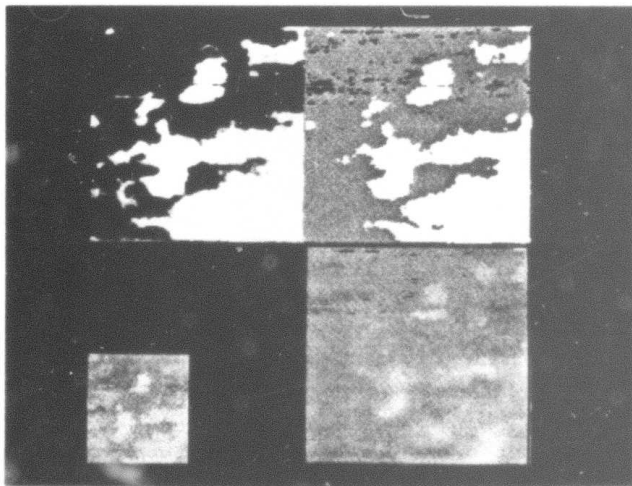
Figure 3:



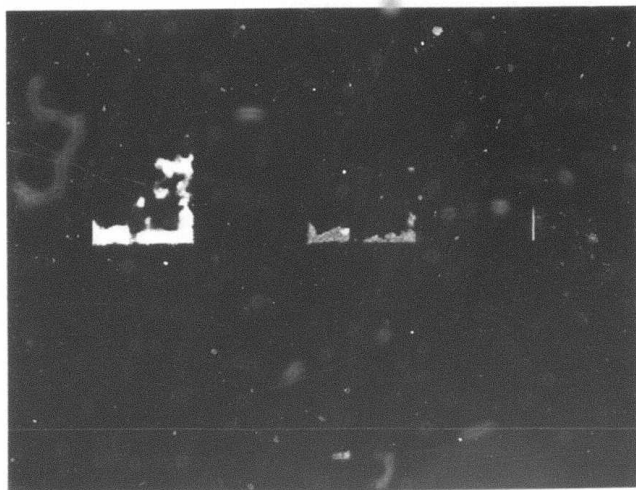
8



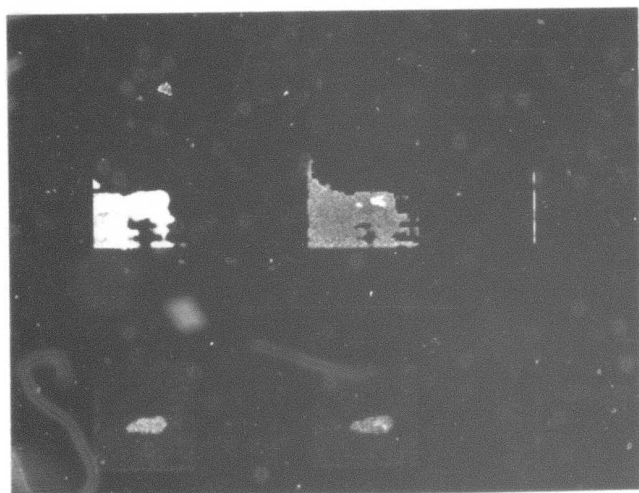
9



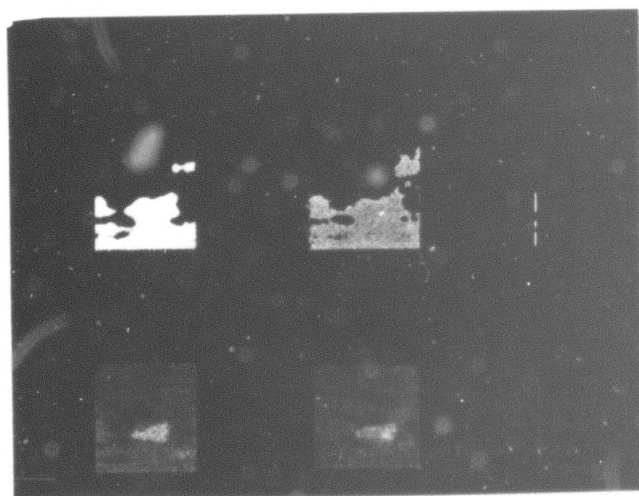
10



11



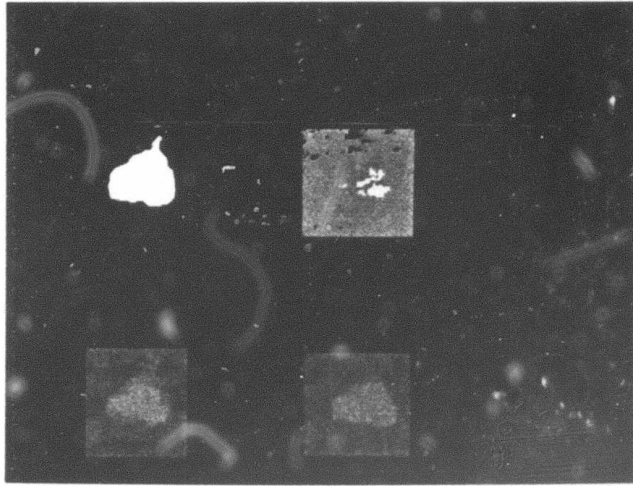
12



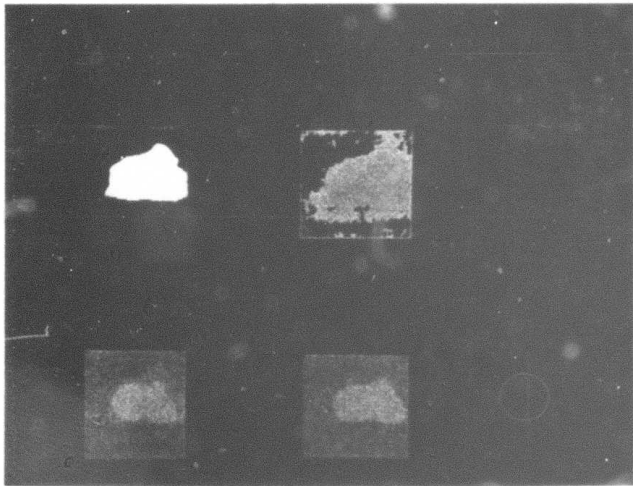
13

Figure 3:

14



15



16

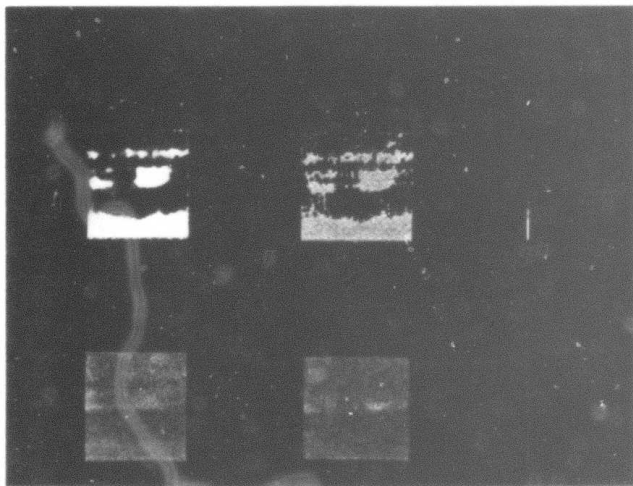
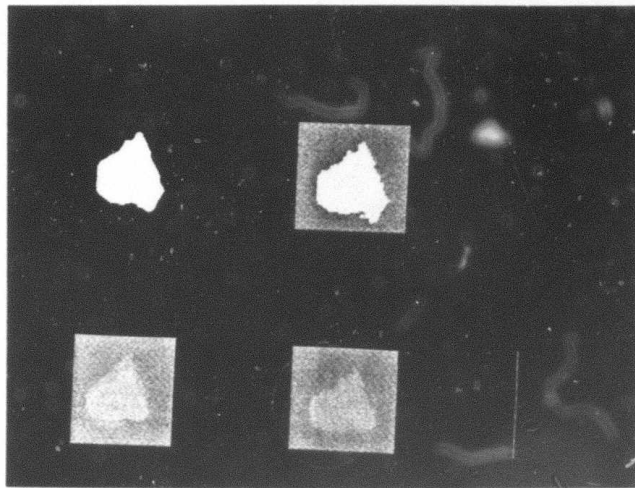
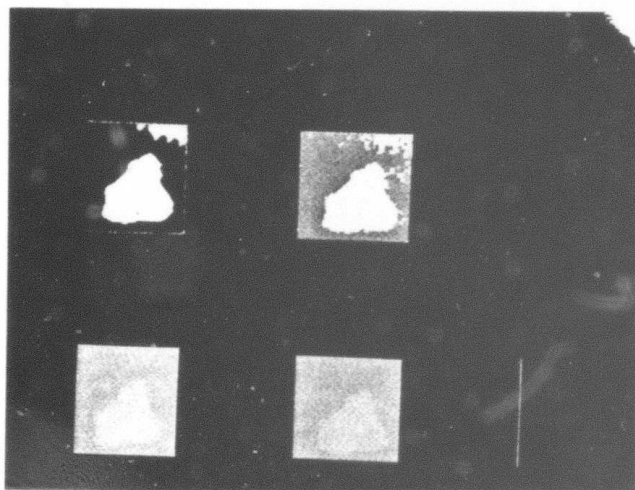


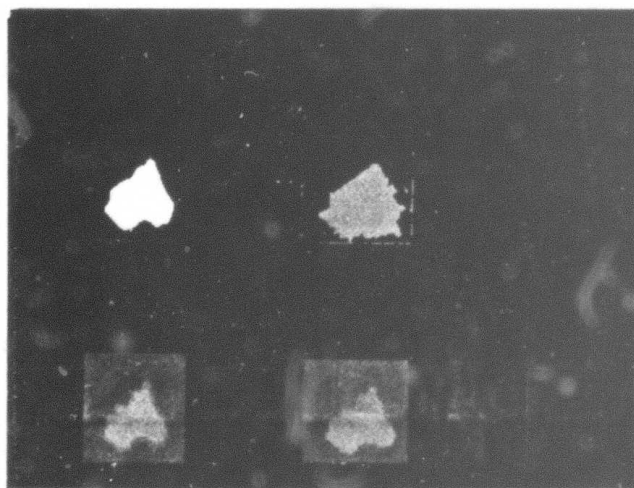
Figure 3:



17

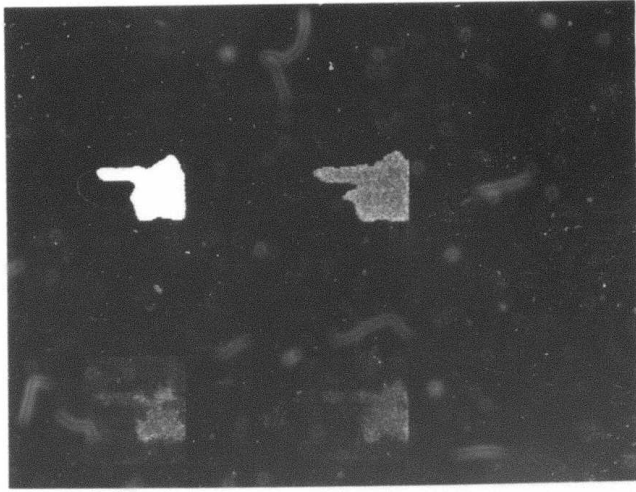


18

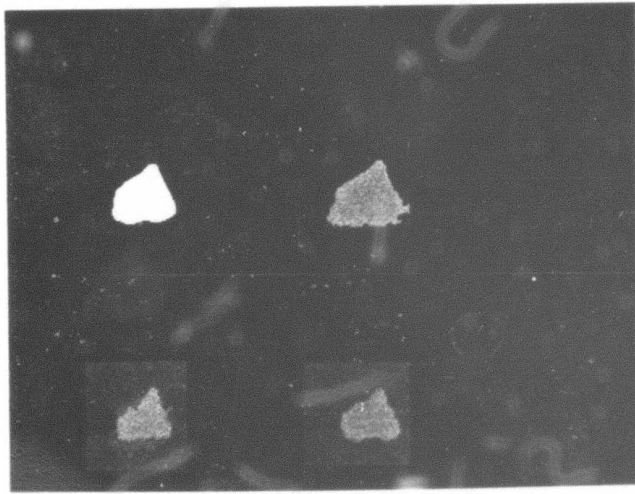


19

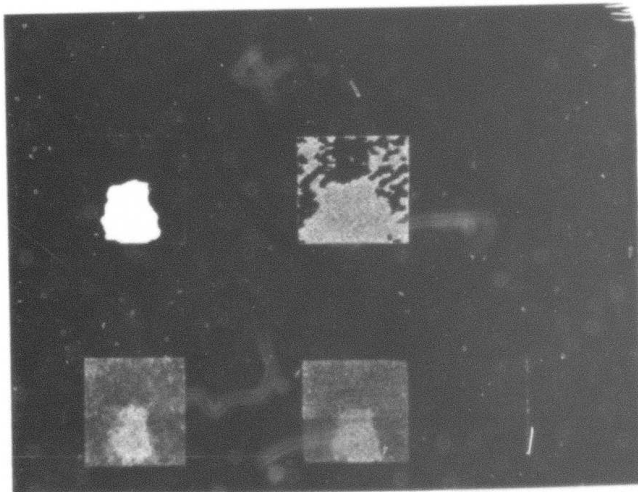
Figure 3:



20

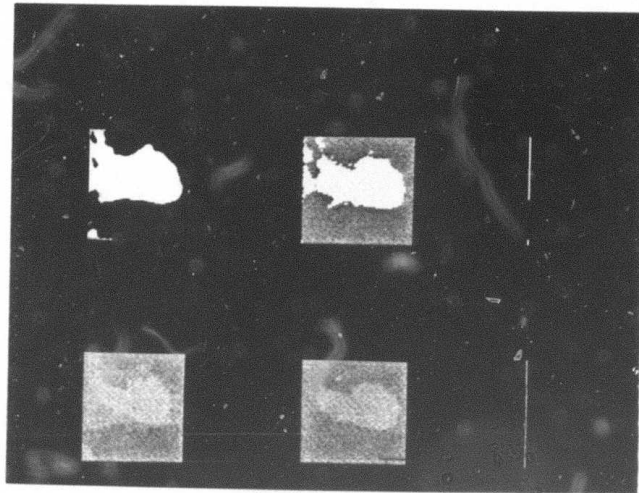


21

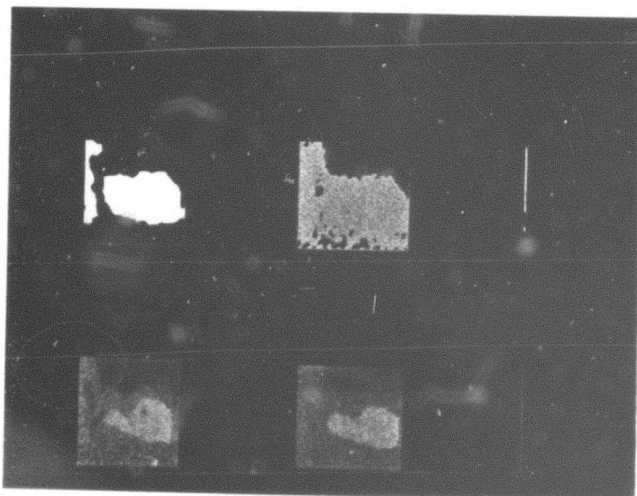


22

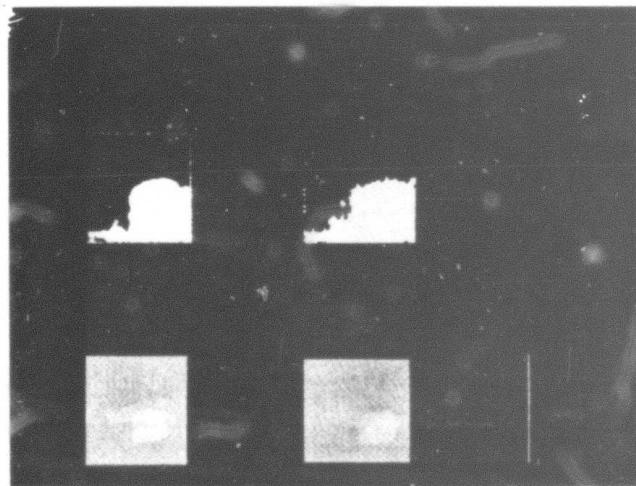
Figure 3:



23

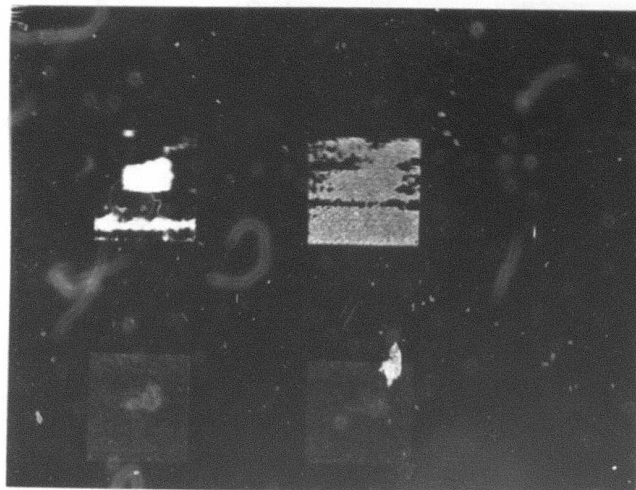


24

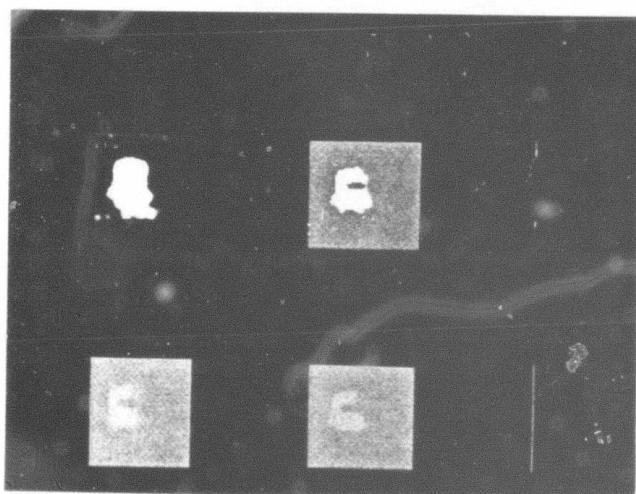


25

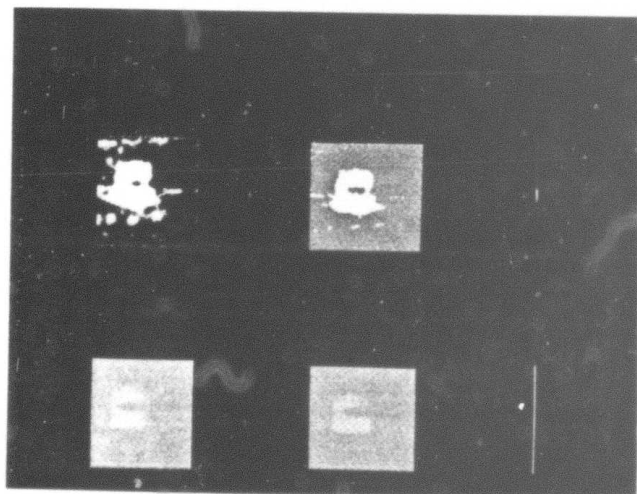
Figure 3:



26

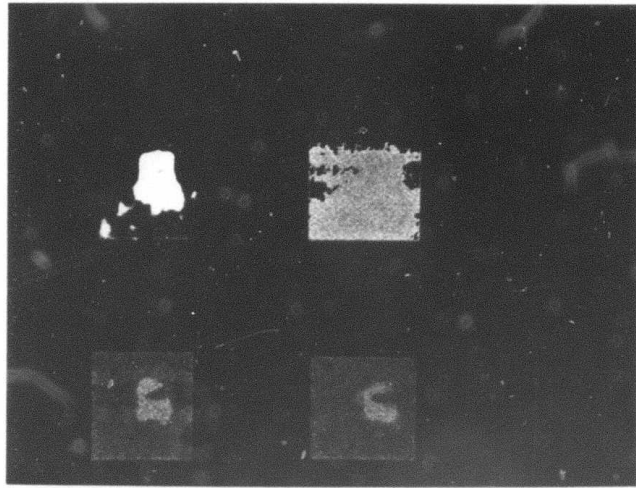


27

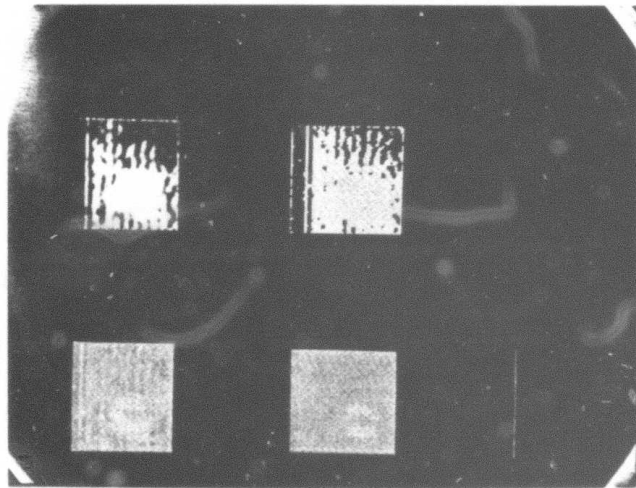


28

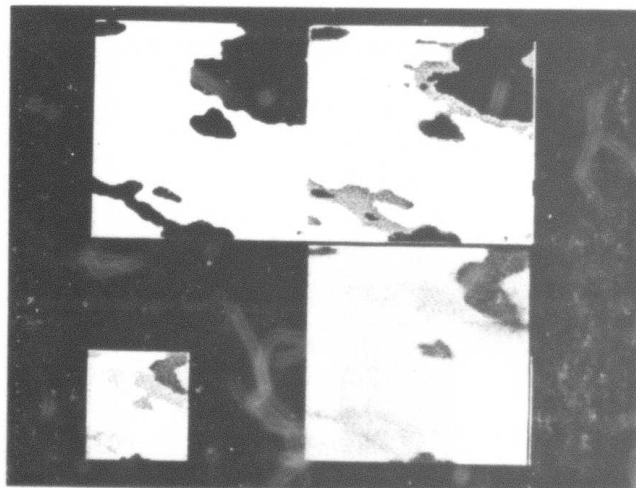
Figure 3:



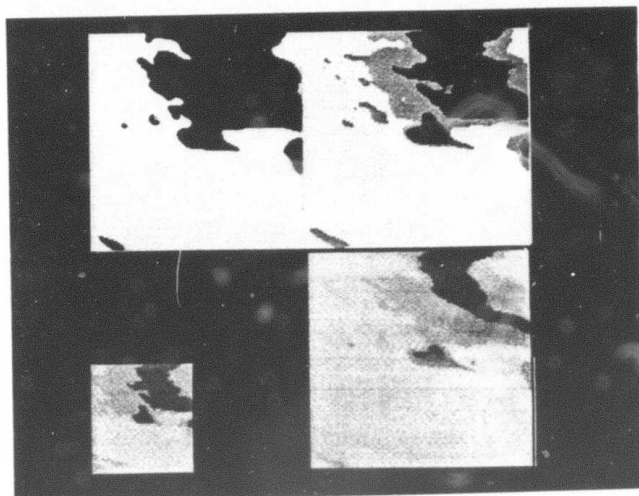
29



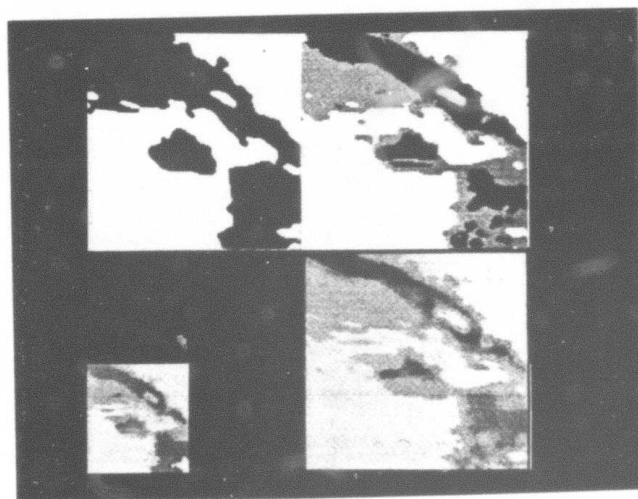
30



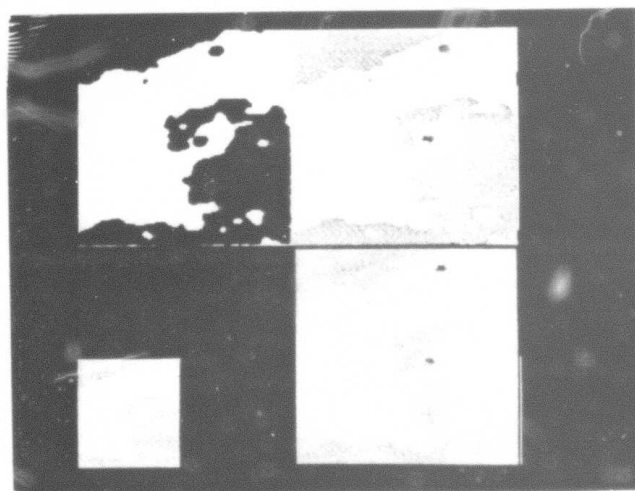
31



32

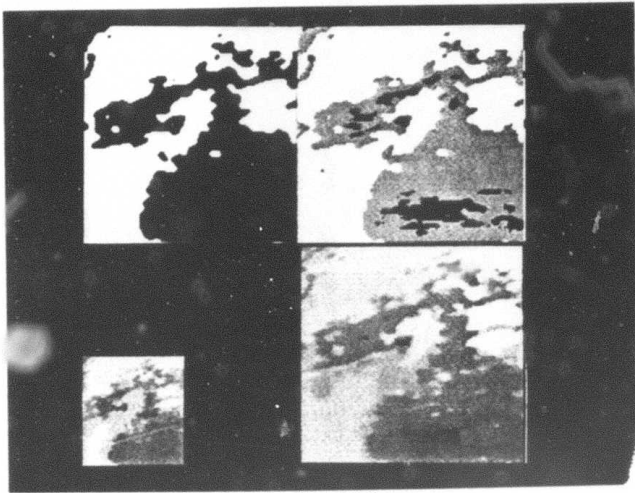


33

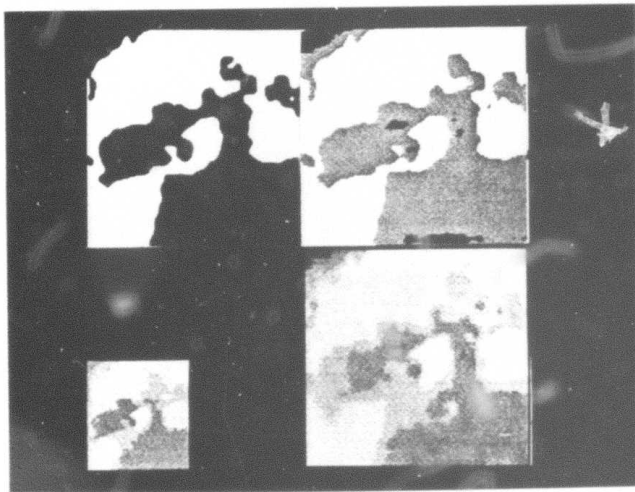


34

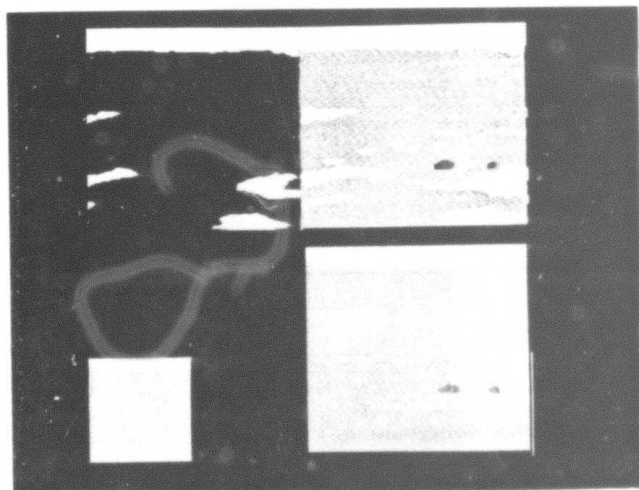
Figure 3:



35

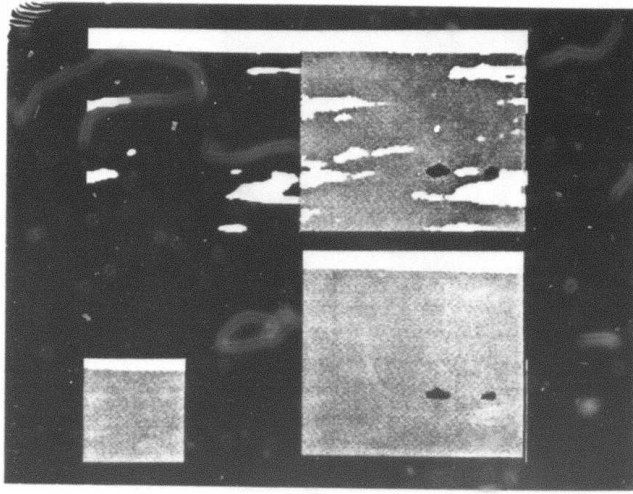


36

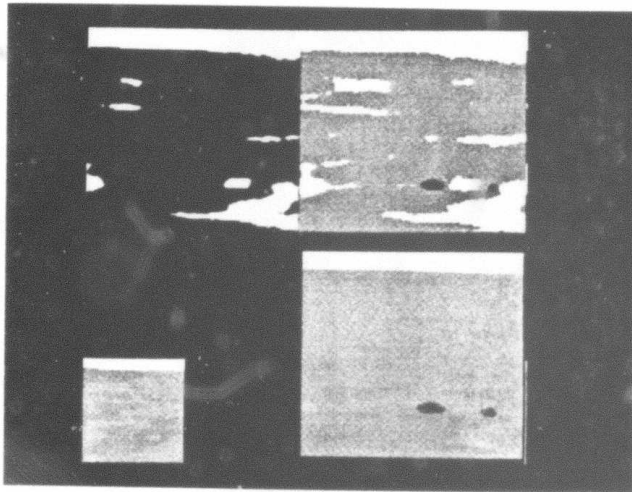


55

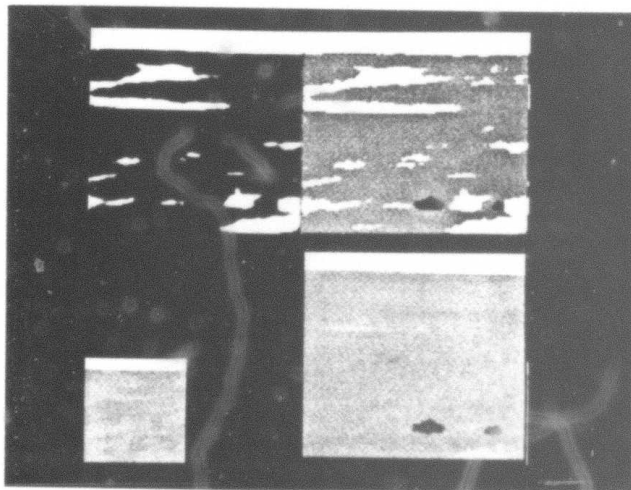
Figure 3:



56

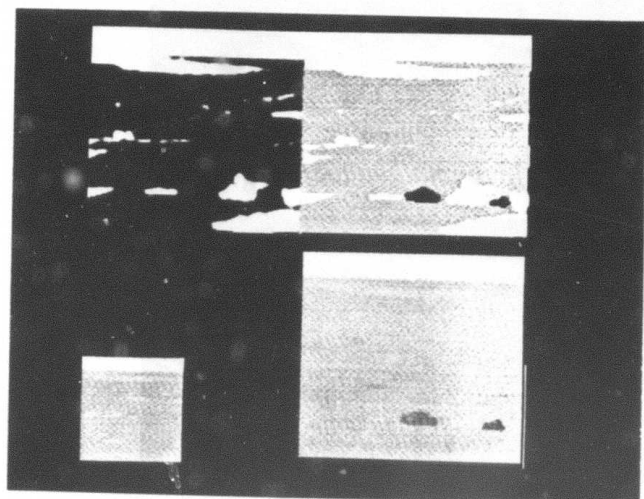


57

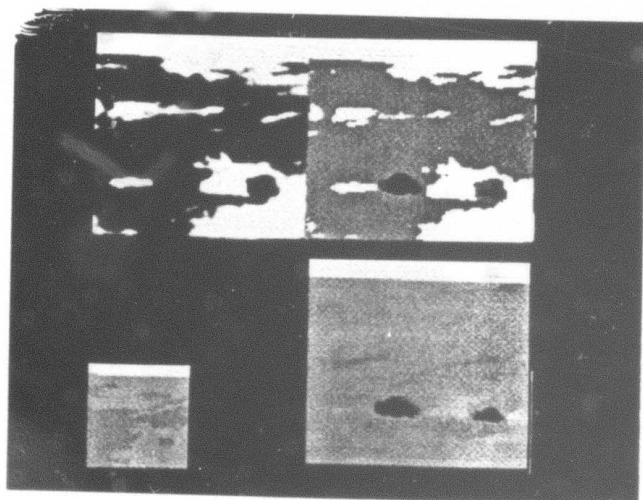


58

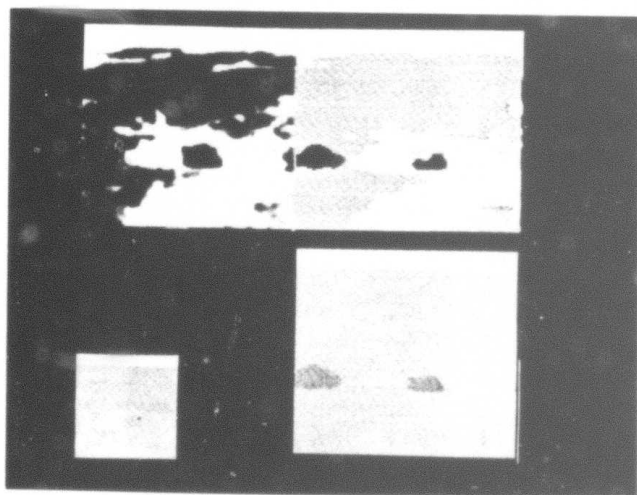
Figure 3:



59

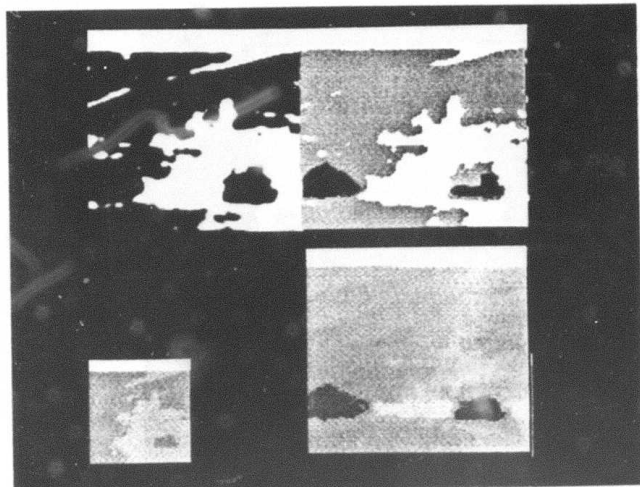


60

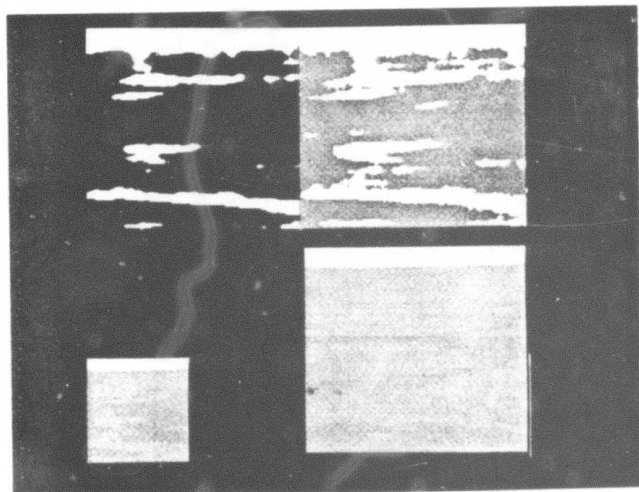


61

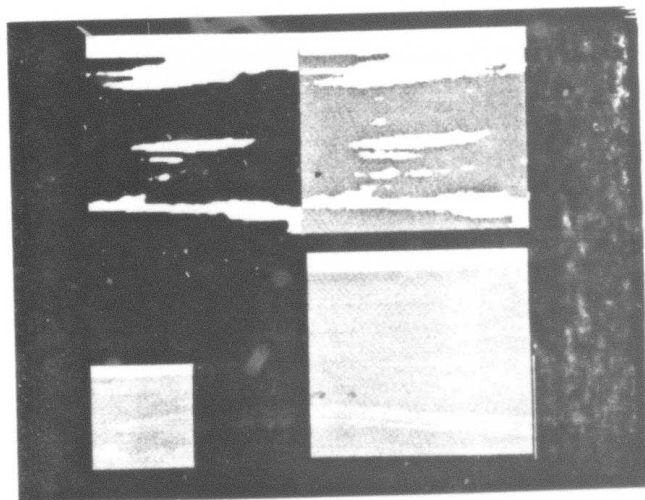
Figure 3:



62

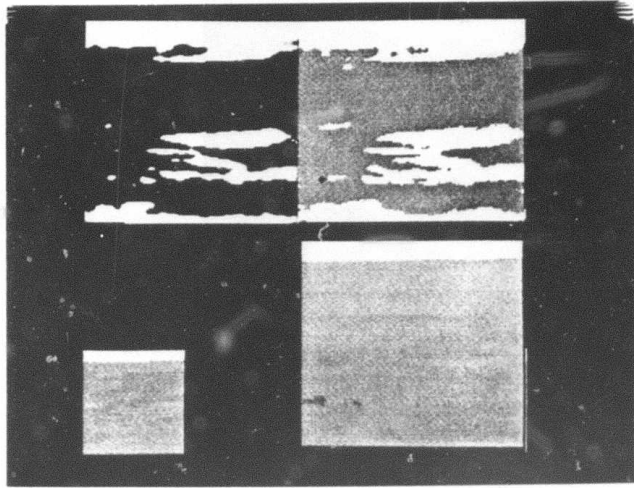


63

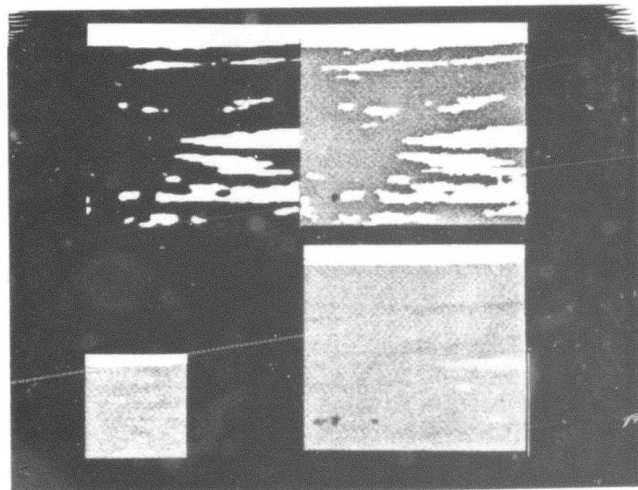


64

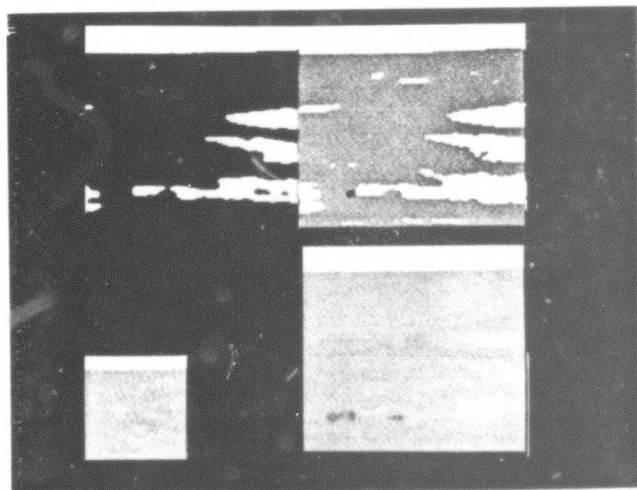
Figure 3:



65

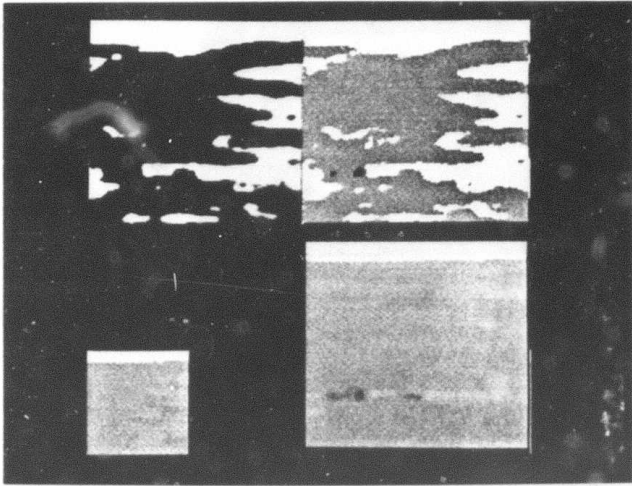


66

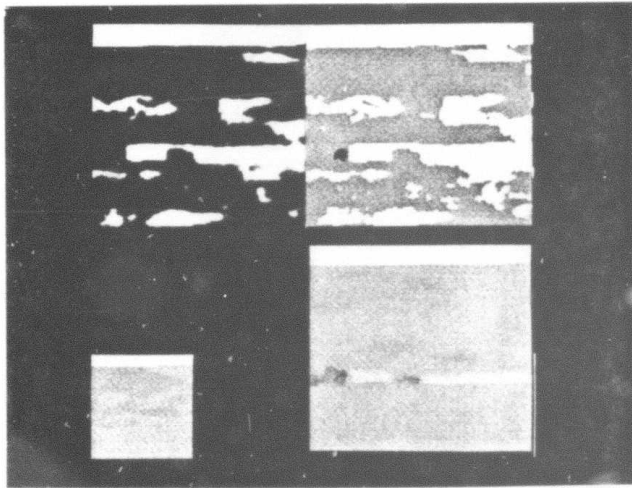


67

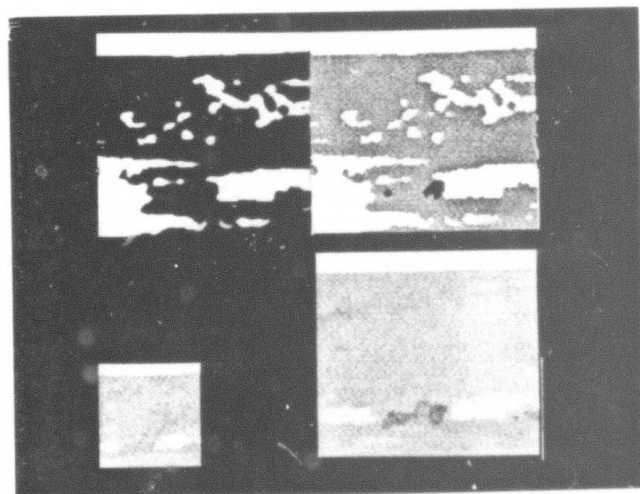
Figure 3:



68



69



70

UNCLASSIFIED

SECURITY CLASSIFICATION OF THIS PAGE (When Data Entered)

REPORT DOCUMENTATION PAGE		READ INSTRUCTIONS BEFORE COMPLETING FORM
1. REPORT NUMBER	2. GOVT ACCESSION NO. AD-A124 809	3. RECIPIENT'S CATALOG NUMBER
4. TITLE (and Subtitle) A COMPARATIVE STUDY OF SEGMENTATION ALGORITHMS FOR FLIR IMAGES		5. TYPE OF REPORT & PERIOD COVERED Technical
		6. PERFORMING ORG. REPORT NUMBER TR-1104
7. AUTHOR(s) Ralph L. Hartley Azriel Rosenfeld Leslie J. Kitchen Cheng-Ye Wang		8. CONTRACT OR GRANT NUMBER(s) DAAG-53-76-C-0138
9. PERFORMING ORGANIZATION NAME AND ADDRESS Computer Vision Laboratory Computer Science Center University of Maryland College Park, MD 20742		10. PROGRAM ELEMENT, PROJECT, TASK AREA & WORK UNIT NUMBERS
11. CONTROLLING OFFICE NAME AND ADDRESS U. S. Army Night Vision Laboratory Ft. Belvoir, VA 22060		12. REPORT DATE September 1981
		13. NUMBER OF PAGES 79
14. MONITORING AGENCY NAME & ADDRESS (if different from Controlling Office)		15. SECURITY CLASS. (of this report) UNCLASSIFIED
		15a. DECLASSIFICATION/DOWNGRADING SCHEDULE
16. DISTRIBUTION STATEMENT (of this Report) Approved for public release; distribution unlimited.		
17. DISTRIBUTION STATEMENT (of the abstract entered in Block 20, if different from Report)		
18. SUPPLEMENTARY NOTES		
19. KEY WORDS (Continue on reverse side if necessary and identify by block number) Image processing Pattern recognition Segmentation FLIR imagery		
20. ABSTRACT (Continue on reverse side if necessary and identify by block number) A comparative study of FLIR segmentation algorithms has been conducted in cooperation with Westinghouse Defense Systems Division. In the Maryland portion of the study, four techniques (two- and three-class relaxation, "pyramid linking", and "superspike") were tested on a Westinghouse-supplied database of 51 images obtained from NVL and other sources. (Two other techniques, "superslice" and "pyramid spot detection", were rejected after preliminary studies.) The best technique, "superspike", extracted regions		

DD FORM 1473
1 JAN 73

EDITION OF 1 NOV 65 IS OBSOLETE

UNCLASSIFIED

SECURITY CLASSIFICATION OF THIS PAGE (When Data Entered)

UNCLASSIFIED

SECURITY CLASSIFICATION OF THIS PAGE(When Data Entered)

corresponding to over 88% of the targets, and had a false alarm rate of 1.6 false regions per true target.

UNCLASSIFIED

SECURITY CLASSIFICATION OF THIS PAGE(When Data Entered)